Complex Infrastructure Systems Analysis and Management, a Case-Study

Niv Yonat[1]
Shabtai Isaak[2]
Igal M. Shohet [3]

ABSTRACT

Complex infrastructure systems are difficult to model. Data is often missing or erroneous, changes are not well documented, and processes are not well understood, on top of it, under complexity, stalwart analytical tools have limited predictive power. The aleatoric risk, such as rain and risk cascading from interconnected infrastructures, is unpredictable. Mitigation, response, and recovery efforts are adversely affected.
In this research, complexity, nonlinear noncontinuous effects and aleatoric and data unknowns, are bypassed by directly addressing systems' response. Graph theory, statistics, as well as Digital Signal Processing tools are applied within a theoretical framework.
A case of a complex infrastructure system is studied. Faults' virtual network is generated, statistics, spatio-temporal behavior and traits are produced. The gained understanding is compared to the physical system's design and to its modus operandi. Implications for design and maintenance are inferred and DSP tools to manage the system in real time are developed.
The contribution of this research is in the provision of an explicatory theory and a management paradigm for complex systems.

KEY WORDS

Climate Change, Complex Infrastructure, Fault Risk, Infrastructure Management, Stormwater Drainage Systems.

INTRODUCTION

Combined sewage and drainage system are cornerstones of civilization, in cities they are Critical Infrastructure. The roman Cloaca Maxima sewage and drainage system was considered "works for which the new splendor of these days has scarcely been able to produce a match" (Livius, AD17). There have been many changes to the practice since the time of the Romans, most notably, the development of rational models. These models which dictate design, are a not a one-to-one procedure, but rather they provide various outcome directed by policies such as sustainability, efficiency, and cost (Aronica & Lanza, 2005). There are well established means to deal with drainage design, maintenance, and operation, which may be presented as three sub-disciplines: capacity design, such as conduit capacity, source control such as delaying, ponding, infiltration, and system management, such as volume reduction by intelligent control (Yu et al., 2017). Computerized analysis enables the incorporation of ever-growing number of influential factors and the integration into the models of correlated systems

[1] Department of Civil and Environmental Engineering, Faculty of Engineering Sciences, Ben-Gurion University Israel. Corresponding author, mail: yonatn@post.bgu.ac.il
[2] Dr., Dapartment of Civil and Environmental Engineering, Faculty of Engineering Sciences, Ben-Gurion University Israel. Email isaacsh@bgu.ac.il
[3] Professor, Dapartment of Civil and Environmental Engineering, Faculty of Engineering Sciences, Ben-Gurion University Israel. email igals@bgu.ac.il
Department of Civil and Construction Engineering, College of Engineering, Chao Yang University of Technology, Taichung, Taiwan, Republic of China.

such as in GIS based threat analysis (Mugume et al., 2015). EU legislative Directive 2000/60/EC for water management directs the coordination of multiple environmental systems into water management such as energy, transport, agriculture, fisheries, regional policy, and tourism with special emphasis on pollutants (Fontaine, 2000). Infrastructure systems are complex systems (Yu et al., 2017). The meaning of “complexity” differs from the literal meaning of being “complicated”. It is a mathematical state that has specific traits and features. These features cause nonlinear system responses such as the butterfly effect that is the effect of small changes that cause large consequences such as manifested in a case-studied by (Aronica & Lanza, 2005) of micro-topography effects of inlets that cause repetitive system collapses. Complexity effects render non-complex design and forecasting tools inefficient (Mullapudi et al., 2017). There is a gap in the understanding of hydraulic drainage systems’ failures in general, let alone under complexity (Zhou et al., 2004). Yet, there is an urgent need for a working tool to manage systems under complexity. Aronica & Lanza (2005) suggest that there are many tools that may compete for this role, if only the flow can be produced. This statement may seem odd when one considers models designed for this purpose such as the US Environmental Protection Agency Storm Water Management Model (SWMM) (Gironás et al., 2010). Aronica & Lanza (2005) explains that assessing flow for a complex topography is impossible and therefore modeling is impaired, this is but of one of many influencing factors such as climate change (Jung et al., 2015), the statistics of deterioration (Salman, 2010) and social factors (Araya & Vasquez, 2022). Can there be a working paradigm under complexity? This article suggests the affirmative. It is suggested to bypass all unknowns and the chaos affected by them by directly relating to system’s response. From systems’ response the systems’ modus operandi may be produced, and corrective and remedial actioned may be generated.

The Response of **C**omplex **I**nfrastructure **S**ystems [CIS], such as stormwater drainage systems response to runoff, is a product of **Morphology** and **Risk** (Yonat & Shohet, 2022a). Spatio-temporal influences produce a complex infrastructure Morphology that generate correlated faults and multiplication and propagation of faults (Yonat & Shohet, 2022b). These effects are heightened by the spatio-temporal variable patterns of rains, which become more erratic due to climate change (Arfa et al., 2021).

Another factor that affects modeling viability is morphological data scarcity and its credibility. Assumptions made upon design become obsolete owing to system morphology changes, coverage changes, permeability factor changes, and climate change (Fitobór et al., 2022).

There are **Barriers** that protect systems from failure (Reason, 1995). Disruptive events, such as flooding, that penetrate the barriers are denominated here “**Faults**”. Faults are generated by factors that are hidden, such as clogging or latent design errors, they are the pathogens of the system (Reason, 2000) and they are largely unknown. Salman (2010) finding that binary logistic regression produces better results than multinomial logistic regression is a manifestation to this. Faults cause cascading disruptions in other systems such as power grids, sewerage systems, and roads (Apan & McDougall, 2015).

All effects and factors that penetrate the system, such as aleatoric risk and risk imported from other systems, cause a response of the system. This response is specific to the system, it forms a behavioral spatio-temporal map of the system. By an analysis of faults, it is possible to generate the system response without knowing the exact morphology, pathogens, and the rain spatio-temporal expression. Faults are the manifestation of the systemic **Risk;** their statistics is a trait of the specific system.

Mourad et al. (2006) analyzed a system as a black box, given all incoming effects and having gauges that produce all outcome of the system’s single outlet, from effluence to BOD, an almost one-to-one function response was formulated and the calculation of the retention tank was a straightforward good practice application. Is it possible to apply similar black box attitude to assess the response of complex systems? Within CIS complexity decides the outcome of events. Under complexity, linear models prove futile because systems response is not linear, finite elements solution produce outcomes such as the Lorentz attractors even for deterministic continuous systems with known initial conditions, where the actual response is not continuous and initial conditions are unknown; simulations are usually prone to modeling mistakes and calibration bias (Mourad et al., 2006), under complexity the problem escalates because the processes are not Markovian in any order and emergent traits are changing the systems‘ overall modus operandi; recursively adjusting systems fail because of the effects of a huge amount of small magnitude events and a small number of big magnitude events; and predictive control (Kändler et al., 2022) succumbs to the butterfly effect and to the disruptive effects of avalanche.

That is why the creation of future scenarios advocated by (Duan et al., 2019), based on a spatio-temporal explicit presentation promoted by (Valizadeh et al., 2019) or a Bayesian belief network (Kabir et al., 2018), or on risk analysis (Johansson & Hassel, 2010), are all urgently called for, and for them to be applicable there is a need for a theoretical framework (Mullapudi et al., 2017). This theoretical framework must be based on a concise paradigm that has an explicatory capacity and may be implemented to direct an application of tools to decipher CIS response, correct their design, and manage them in real time.

Addressing these needs is the aim of this research.

In this case-study a municipal drainage system is analyzed. It is used to present concepts of the Theory of Faults [ToF (Yonat & Shohet, 2022)] which is a paradigm for complexity, to show that complexity is in the aleatoric risk, in the system morphology and as a result in the system response, and to present inferences and tools for forecasting and for reevaluation of design and to support the development of real-time tools.

DEFINITIONS and CONCEPTS

Nodes -[here] Conduits in the physical system, faults in the information network.
Edges -link between nodes, the edge retains the timeline and WBS.
Rank - the number of nondirected edges emanating from a node.
Outdegree - the number of outgoing edges emanating from a node.
WBS/Tree - **W**ork **B**reakdown **S**tructure the breakdown of a conduit to its supply lines.
DSM - **D**esign **S**tructure **M**atrix where [here] horizontal entries are "from", vertical are "to".
Adjacency matrix is a DSM weighted by physical parameters such as resistance or capacity.
Viability Kernel

$$x(t) \in K \quad (1$$

$$\dot{x}(t) \in F(x_i(t)) \quad (2$$

Here x is the actual routes vector [state variable], $x_i(t)$ are the stage variables $F(x_i(t))$ is the decision function.

Attractors are paths that the system tends to prefer. Attractors act as minimum/maximum energy states that a net prefers under the excitation of a fault wave. PCA analysis shows that attractor are not paths but rather nodes (Yonat & Shohet, 2022a).

Hub -nodes with a high betweenness centrality.
Risk -[here] refers to Faults **P**robability **D**istribution **F**unction [PDF].
Aleatoric Risk Generators -such as [here] rain.
Pathogens -clogging, sagging, air pockets, inlet capacity, hydraulic shock, background concentration, etc. Pathogens are caused by aging, inadequate materials, bad workmanship, latent design errors, etc.
Complex morphology -when nodes' rank has a power function and small world effects emerge.
Synchronization -In network analysis a loop is considered synchronized.
Avalanche: -when a local effect progresses the system to infinity [here to its edges].
The Butterfly Effect -when small perturbations cause unlimited effects.
Digital **S**ignal **P**rocessing -[DSP] digital=numeric. Tools for system analysis and management.

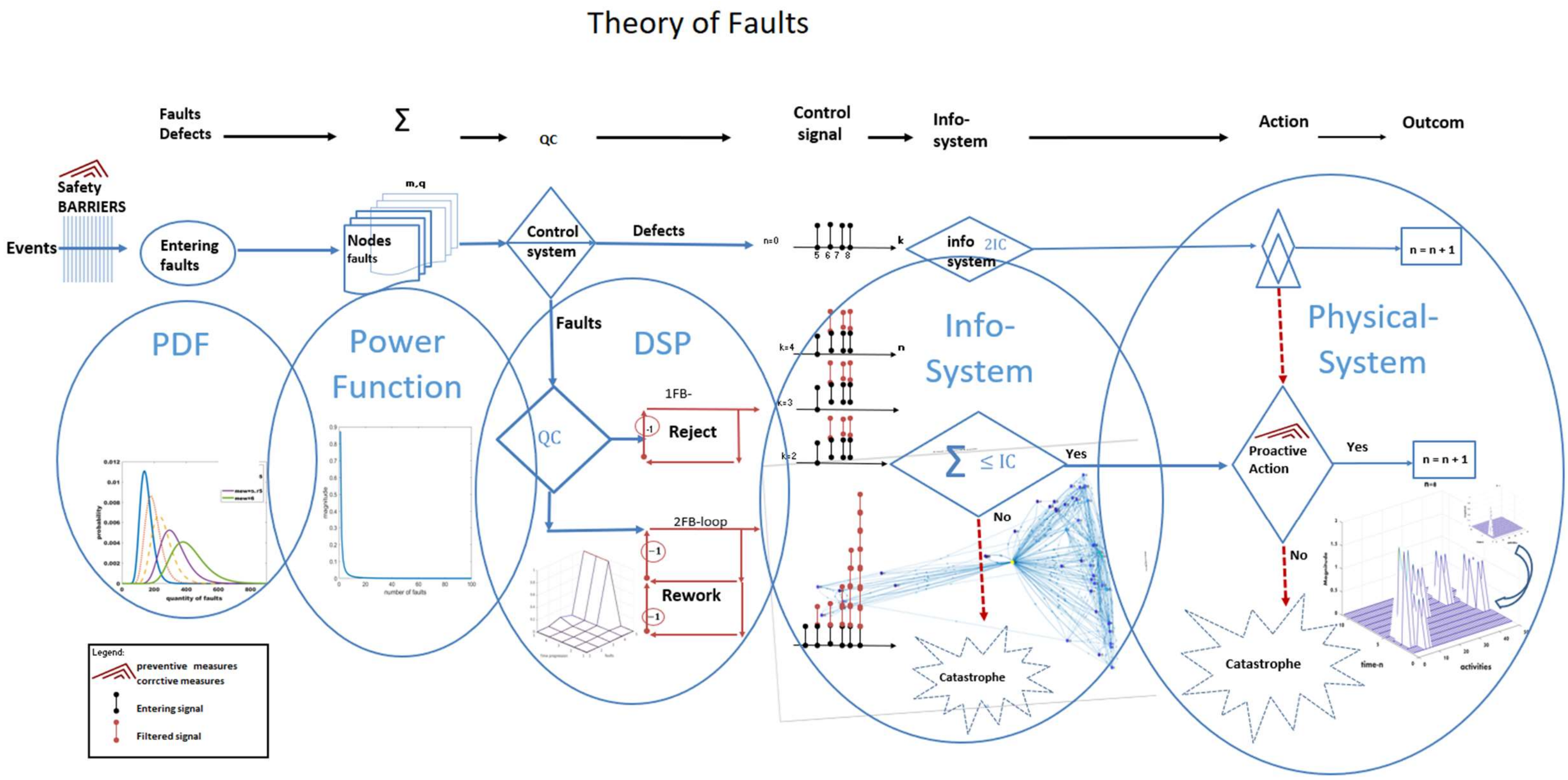

Fig. 1. Graphical abstract of Fault propagation through the system

System response [here] to flows. The response is a product of the system's morphology.
Barriers such as standards for materials, praxis for workmanship, specs for suppliers, peer review for design, timely maintenance, and regulations,- prevent aleatoric risk translation to fault by weeding out causes of pathogens and by removal of pathogens.
Faults here are reported events related to drainage such as sagging, flooding, cover lifting etc. Fault may be generated by bad workmanship, materials deficiency, design mistakes, municipality maintenance actions and omissions, and so on. Faults may generate responses in the info-system. Once barriers are penetrated, the info-system has its chance to stem the faults at inception, otherwise, faults propagate, magnify and multiply to avalanche.
Open faults and only open faults generate overflow. Morphology multiplies, inflates, and propagates the faults.
Faults PDF is log-normal (Horvath, 1959). The aleatoric risks are translated by the system to fault PDF.
Faults magnitude has a power function (Yonat & Shohet, 2022b).
Power function is generated by the log-normal PDF (Yonat & Shohet, 2022b), it is scale free; therefore, the same function provides for time, cost, and magnitude of faults with only a change of a scaler.

METHOD

The article employs an empirical approach (Johansson & Hassel, 2010).
A case-study of a municipal drainage system is studied.
Rain depth data is analyzed for the duration that matches the case-study data. The **Rain depth PDF** is generated and analyzed. **Faults PDF** is generated, **Faults'** magnitude **Power Function** is produced. **Fault** spatio-temporal **network** is developed. It is compared to the physical systems parameters, such

as topography, roads, conduits. The physical system is analyzed by various tools of **descriptive statistics** and by DSP tools. The understanding is used to produce intake for design and design corrections, and to develop **DSP controllers** to automatically manage the system.
The layout of this article is:
Following the **Definitions** and **Method** section, the research **Hypothesis** is presented, further on, in the **Results** section, the presentation progresses along Fig. 1 trajectory from PDF to Power function through descriptive statistics and DSP analysis to a generation of faults networks and the application of those to the physical realities of the case. Derived are morphology spatio-temporal maps, complexity effects, synchronization, attractors, and eventually DSP controllers. The **Discussion and Summary** section follows with further insights and inferences. The **Conclusion** recaps the findings, and the contribution of this article.
The numerical data, morphology, statistics, explicatory parameters, and results are documented in the **Appendix.**

RESEARCH HYPOTHESIS

Physical infrastructure systems are a product of higher order information systems.

RESULTS

Rain Depth Characteristics

Daily rain thickness timeline data [Fig. 2] indicate that the municipal stormwater drainage system master plan design assumption of smooth concave stratified rain functions [Fig. 10.6] is irrelevant. The same erratic non-smooth behavior was found on the spatial axis too [Fig. 7]. The meteorological station located but a few km away, that produced data that was used for many years, no longer represent the rainfall of the studied municipality [Fig. 7].
Fig. 2 lays out a 7-year aggregated rain-thickness Histogram, a PDF fitted by Matlab statistics app., a rain-thickness time-line graph, and a rain frequency/amplitude graph generated by Fast Fourier Transform [FFT]. The Histogram shows that entire depth sections are missing, for example, within 7 years there - of 80 mm thickness. The rain thickness fitted PDF is non-parametric [Fig. 2.2]. There is roughly the same probability for 20- and 40-mm events and a 350 mm event. Events of 350 mm have not been recorded yet, but above 100 mm events have become a probable occurrence, much like a 50 mm events. The 7-year daily rain graphs presented on shared ordinate scale of ordered ordinate, show a chaotic pattern [Fig. 2.3]. The FFT is a manifestation of chaos [Fig. 2.4]. There is similar probability for different frequencies. This is a falsification of the [Fig. 10.6] concave rain-depth probability paradigm.

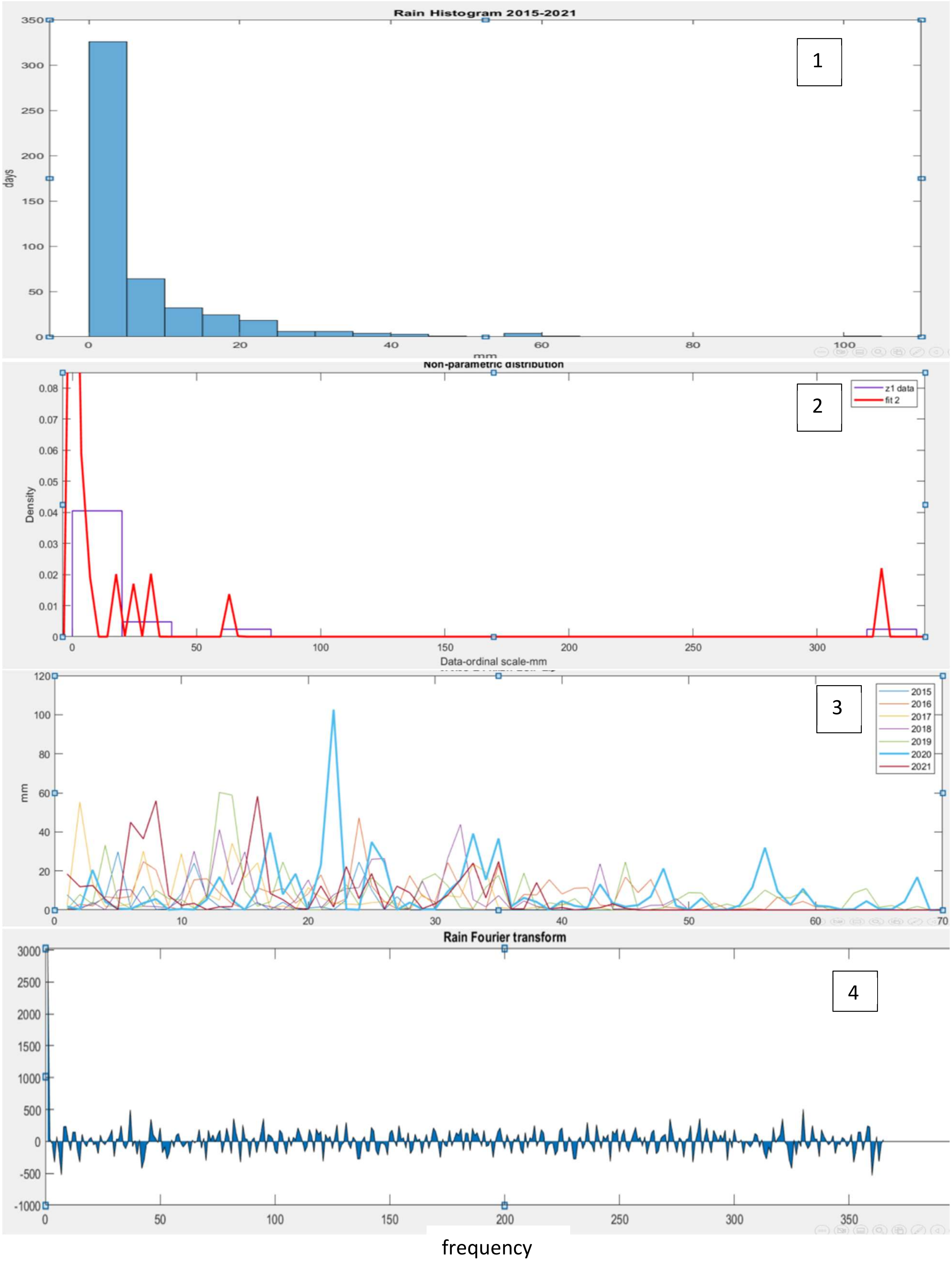

Fig. 2. Rain attributes by 1.rain histogram in mm, 2.rain PDF, 3.rain scatter plot, 4-rain FFT

Fault Statistics

The municipality report center notes all incoming complaints, sorts them by discipline, weeds-out redundancies and sends a professional to verify each report. The Appendix archives verified stormwater drainage system related reports on Fig. 8. The data log documents about 22,700 verified drainage related reports acquired in less than 7 years. The shear amount is an indication to avalanche. The data supplied by the report center was sorted by the center according to 4 fields: Date-Time of opening a complaint, Date-Time of closing a complaint, location, and nature of fault [Fig. 8]. Per the data, there are no open faults, ostensibly every known "pathogen" is meticulously weeded out. Active pathogens are hidden.

The physical system hydrologic parameters are taken from the master plan hydrological data [Fig. 9], this data is partial and based on assumptions [such as coefficient of imperviousness, conduit fill rate, Kirpich coefficient etc.]. Some hydrological considerations [Fig. 10] were taken from the master plan to show that the system is by no means capable of draining the city, even in case of the design storm.

Some spatio-temporal descriptive statistics is presented on Fig. 11. Timeline Histogram shows a probable avalanche in 2019 that permanently altered the system's response for the worse. Street flooding percentage of total expectancy [Fig. 11.3], point towards possible attractors, and the Pareto diagram of streets Faults' expectancy [Fig. 11.4], shows that 10% of the roads sustain more than 60% of the faults, while 20% of the roads are a locus of about 90% of the documented faults.

Fault PDF is presented on Fig. 3. Lognormal PDF was found to have a good match, as provisioned by the literature (Horvath, 1959), and experience (Yonat & Shohet, 2022b).

The PDF was generated by Matlab statistic app. For 95% confidence interval [Fig. 3].

The FFT of the Faults log shows repetitive formations consistently covering the whole ordinate.

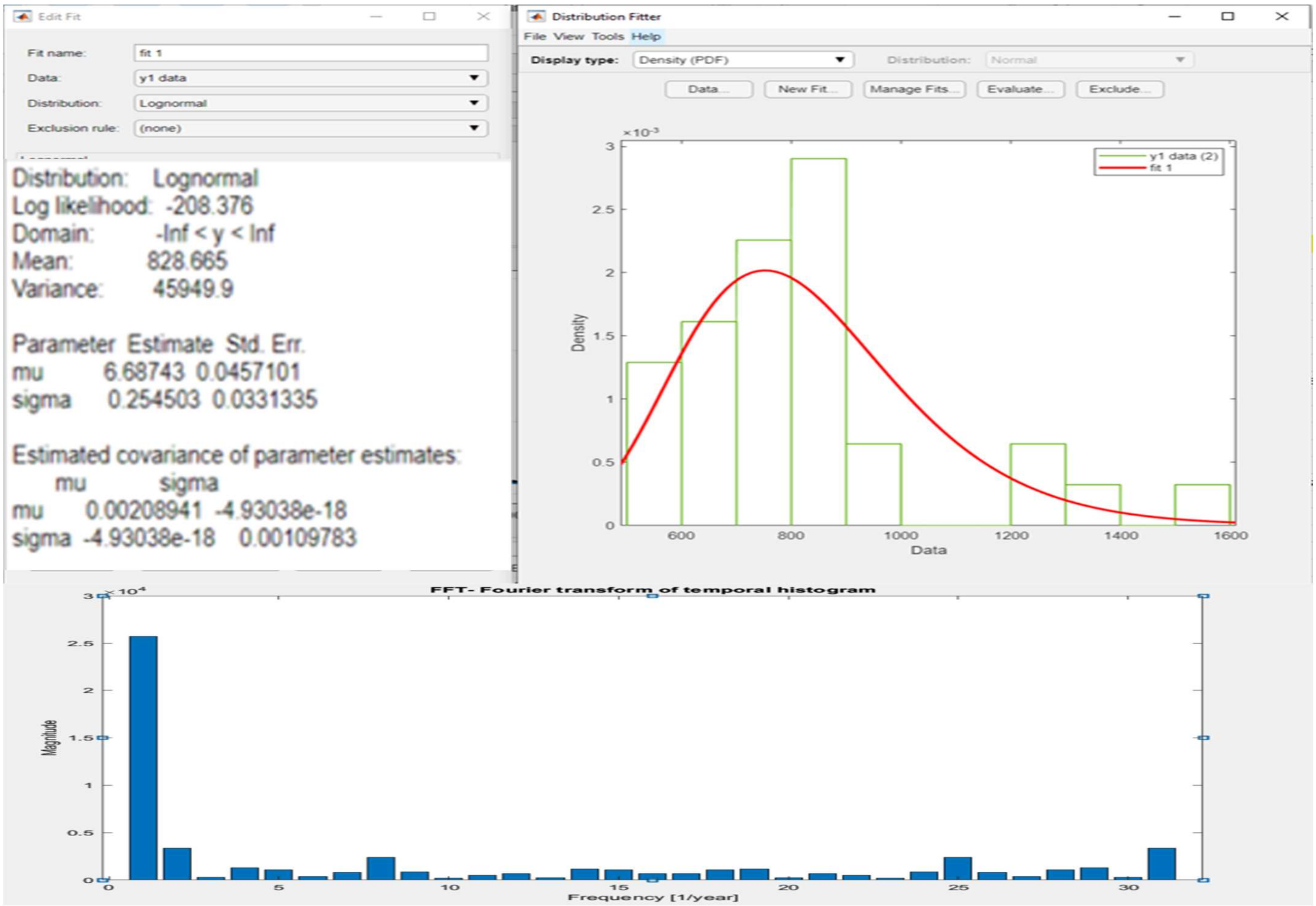

Fig. 3. Matlab generated 95% confidence interval faults PDF and FFT

Curve fitting Matlab app. found power function [a*x-b+c] to be the best fit [95% confidence interval, R^2=0.96] for representing the magnitude of the faults [Fig. 4].
Abs(b)=0.4 complies with avalanched projects and infrastructure facilities.

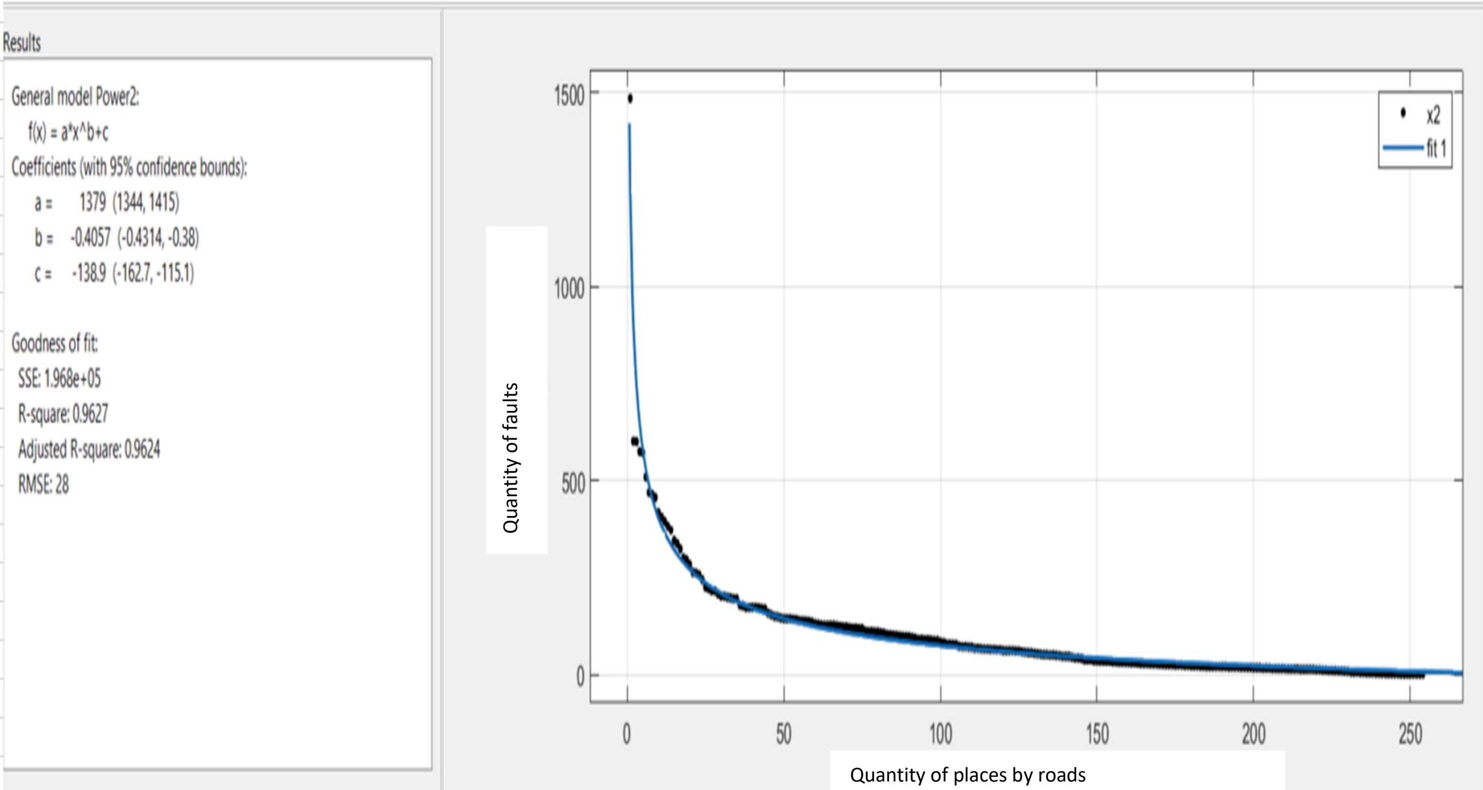

Fig. 4. Power function fitted by Matlab app.

The power function exhibits a trait of constant "noise" [
Fig. 15. The cause of the White noise
]. This noise is called "White" when its attributes are not correlated with those of the magnitude of faults. White noise can be random, or it may have a repetitive trend such as the one exhibited on
Fig. 15. The cause of the White noise
. The origins of the white noise were investigated and traced to an avalanche in the sewage system in 2018 that caused a permanent effect on the system. This sewage system major fault was correlated on
Fig. 15 with an avalanche in the drainage system a year later, causing a permanent effect. Power functions are formed in almost any spatial analysis such as on Fig. 16.3 which is a spatial presentation of one specific fault, and on Fig. 11.3 for the aggregation of all faults. One may infer that the power function of Fig. 11.3 is broken down to smaller power function forming fractals on any axis, such as the fault type axis chosen for Fig. 16.3, or vice versa, that local power functions are aggregated by the complex system to super power function. This is a manifestation of correlation of faults, of complex propagation modes and of superposition of vibration modes.
Fig. 5 shows that the stormwater system is flooded also in the summer when there are no rains. The initial supposition that it is flooded by wash water deposited by summer pumps was rejected because the complaint log clearly indicated sewer. The deposition of sewer into drainage systems is illegal in

Israel, perhaps that is why failures cascading between these infrastructures were not considered and patterns related to its correlated failures caused by interdependencies were neglected.

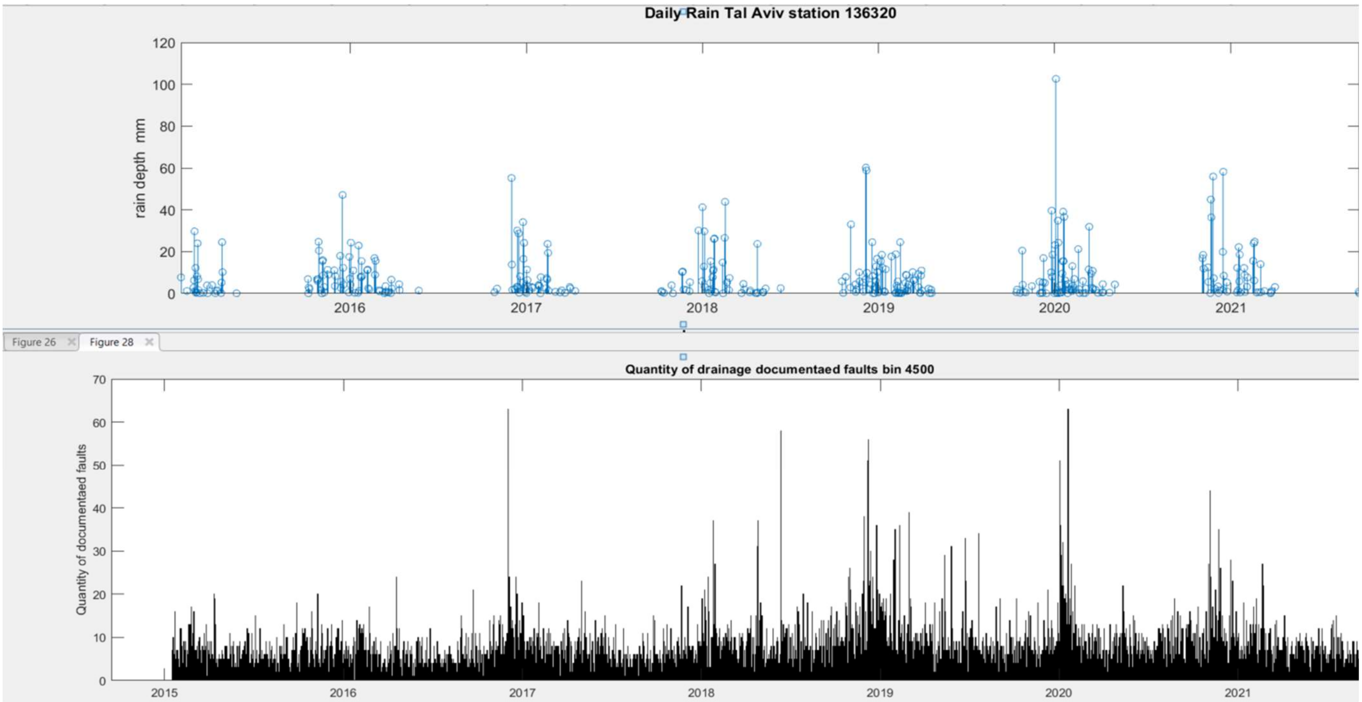

Fig. 5. Rain timeline vs. flooding timeline. Histogram accumulated for 10 hour spans.

System Morphology

The municipality occupies an 8 sq.km watershed adjacent to the Mediterranean Sea. The general topographic inclination is towards the sea, to where the western outlets are directed [Fig. 9]. There are three main catchments: East, N. West and S. West.

The municipal drainage system is a Critical Infrastructure, affecting service, cost and on rare occasions causing loss of lives. There are cross effects with other infrastructure systems, in this case-study with the sewerage and road systems [

Fig. 15].

There is only partial data about the physical system, even this data is rendered irrelevant because the planned and executed system is modified, clogged, sagged, conduits are fractured, their gradient changed, there are illegal addition especially of sewage connections and relentless densification caused changes in the coverage and permeability factor.

Aleatoric events that penetrate the barriers become Faults.

Faults create virtual networks [Fig. 18, Fig. 6, Fig. 19]. These networks are spatio-temporal. The plots were generated by Matlab from the adjacency matrix.

The nodes are faults, the edges are propagation trajectories. The scale can be enlarged to view a specific rainstorm such as on Fig. 6, or zoomed out to show the system general morphology such as on Fig. 18.

It is evident [Fig. 18] that the system consists of Hubs, it has subgraphs with modular repetitive hierarchies, and there are incidents of coupling. It is important to weigh the network against the viability kernel, to evaluate edges that may present a queue in the complaint center rather than ones in the drainage system.

The western parts of the system have only three outlets [Fig. 18]. The calculated capacity of those outlets (Fig. 9), gives us a gross estimate of the total capacity of the system. Total catchment area for the N. Western outlet is calculated in Fig. 10.4 for a rain of the designed concentration time and total

volume Fig. 10.1. The calculation assuming the system averages on one outlet for that catchment yields a time for clearance that is at least on order of magnitude bigger than the actual one [Fig. 10.1], thus falsifying the assumption that the drainage system drains the city.
Fig. 6 presents a recurrent emergent trait of water flowing under pressure against the gradient, flooding uphill locations. In this case water travelled 8 km upstream flooding the areas along rout. The white dashed arrow on Fig. 6.2 shows the farthest reach of the phenomenon, which is the farthest extremes of the net. This is an avalanche.

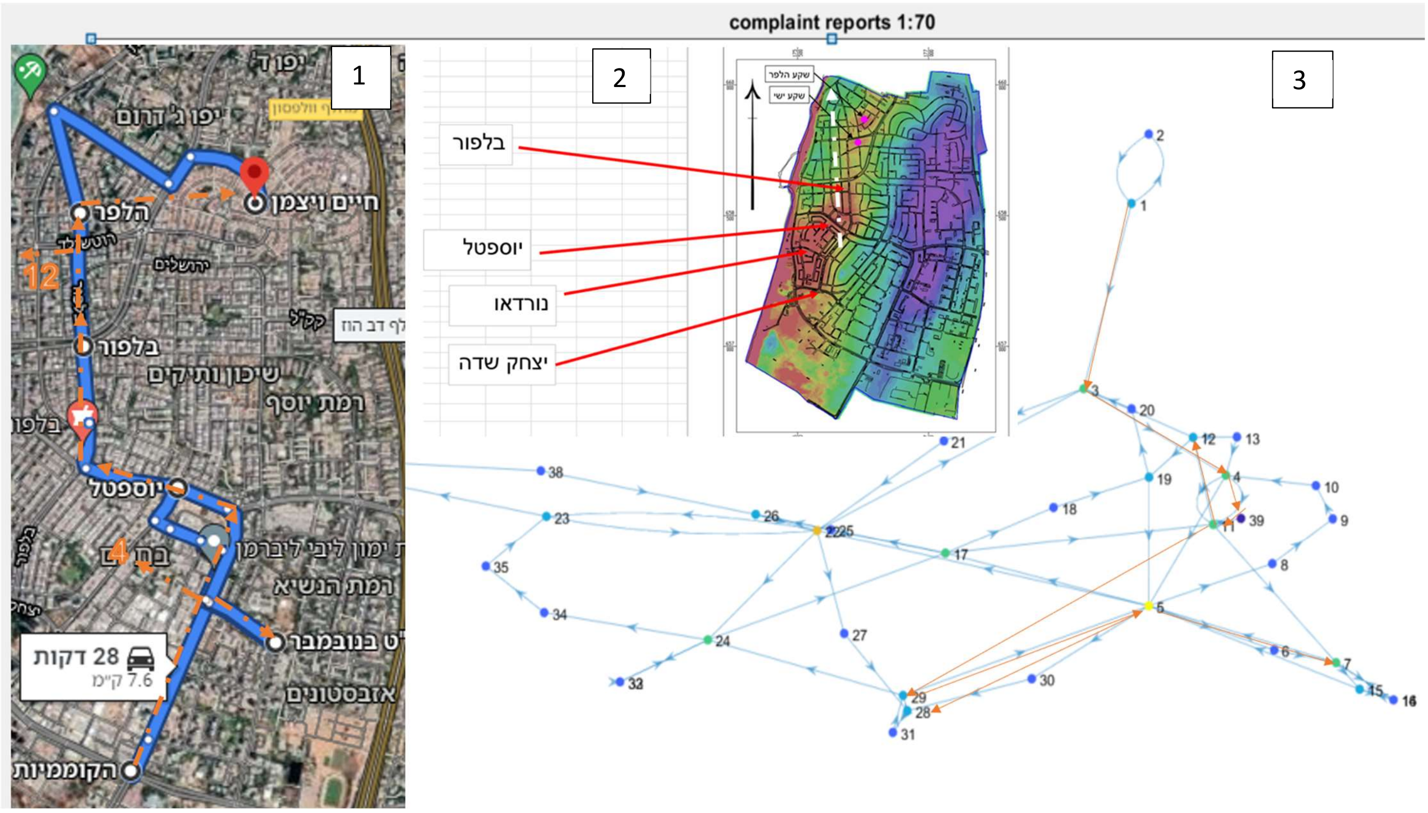

Fig. 6. Partial virtual faults network (1) vs. physical conduits (2) and topography (3)

Node 1 on Fig. 6.3 is the first [left most] on Fig. 16.3. Weather this pressure vessel is the power engine of this pressure system or its outcome may be suggested from the fact that cover burst and pressure discharge do not change the trajectory of the pressure system, on the contrary, it preceds it.
Fig. 19 presents the role of a hub.
This hub [highlighted on Fig. 19.3] generated a “black swan” event of flooding of the adjacent uphill catchment [colored in pink on the topographic map Fig. 19.1]. This water main [hub] on the low catchment has a root in the adjacent uphill catchment (circled with a dashed line). Water velocity and pressure forced the pressurized transport of floodwater from the low adjacent catchment to the upper one. The explicatory model is presented on Fig. 19.4. The pressure in the main is higher than that of the supply pipe, thus water in the supply line is stacked to the height of the water in the main, this stacking goes up the conduit according to the height pressure. Water that flows above that level can pour into the main. When water level in the main is above TL of the supply pipe, water flows under pressure to be siphoned out of manholes according to Bernoulli equation [Fig. 16]. Air pockets in the sewage system are formed, hydraulic shocks, turbulence, hydraulic jumps all contribute to the chaotic response. Water streamed up the dashed vertical lines of Fig. 19.3 in sequence, and only after filling the dashed conduits, the uphill effect is created. These are design errors traced by Fig. 19.4 to wrong Invert Levels of conduits.

In the western part of the catchment presented on Fig. 19, the land is flat and average gradient is 0.3% at most. This causes invert levels [IL] to be roughly the same for all conduits in a manhole. For the same effect to appear when invert level of the supply line is higher than that of the main, a flooded manhole and a main that is full and operate under pressure is needed [Fig. 16.2 Fig. 17.3 respectively]. This main conduit acts as an attractor, meaning that it is flooded in many instances. The flooding surfaces through gutters and manholes to the ground, in the same specific locations, which are the manifestation of that attractor. Their flooding is the system choice. These attractors are expected to be flooded when different aleatoric events happen and different pathogens such as clogging or sagging of manholes are active in different placed.
Loops are formed on a system level such as the grand loop leading to node 3 in Fig. 19, and on a local level such as the coupling of nodes 31 and 67. These loops indicate higher topologies. A salient example is formed on the northern extreme of the main in Fig. 19.1, where the two local recesses are located [their perimeter is noted by a solid red line]. This location is zoomed in on the Fig. 19.3 to show the emergence of a coupled tank system- an oscillator.

DSP

Some DSP controllers were developed for sections of this case's physical system and for the management of the recesses. Perhaps the simplest most forward one is a PID controller suggested on Fig. 20. The idea is to create a seasonal pond in the noted location, taking in the adjacent flows [represented by double blue arrows], thus relieving the system. The soil is sand, therefore there is a considerable infiltration [the parameters are noted on Fig. 20]. All the flows are gravitational but one. The pump location is noted. The pump is needed because a block in the system is formed at this junction owing to a Bernoulli effect of velocity and pressure [Fig. 19.4]. The pump role is to over pump the main, thus, to reduce the pressure up the conduit and relieve the system further upstream. There is an overflow slide [noted in orange arrow], that is a safeguard for extreme events of flooding. The system works as a crude surge tank because the junction noted with a red ellipse on Fig. 20 is blocked when the system is flooded, and backflows are directed to the pond.
The only sensor used is a water level gauge for the pond. This is in essence an integral indicator. Thus, the effect on the PID design parameters [Fig. 21] is the almost nullifying of the Integral part of the PID controller.
The PID was developed in Matlab Simulink control system toolbox [Fig. 21]. PID function had to be limited to the capacity of the system and the pump, consequently making the control a safeguard measure. Water level gauges provide Integral, velocity may be a measure of Derivative while in other formations, flow may indicate the Proportional. In some cases, it is possible to substituted a DSP tool for a Feedback loop. An example for a simple feedback system: in section 14 of Fig. 19.3, the pink rectangular dot represents a "summer" pump that pumps excess water into the local main which has a branch into the Halper [upper] recess. A controller may be added to close that branch by a valve when Halper height gauge indicates water level above a set height. This is a simple proportional management. This logic may yield sub-optimal solutions when the Halper pump capacity is sufficient to sustain the flows. A different approach is a feedback loop that returns the pressure against which the pump works. This approach is better because the main conduit flooding is a precursor of the recess flooding.

DISCUSSION and SUMMARY

CIS are produced by information systems, that is because CIS are built according to design. CIS are operated and managed by information systems, and it is information that dictates CIS maintenance. CIS produce and feedback information, falsification, and validation into info-systems. These are systemic characteristics; they were repeatedly presented here. These systemic characteristics support the research hypothesis.

Owing to climate change, rain characteristic changed considerably relative to the municipal master plan database. Rain patterns are spatially and temporally different. It was found that rain behavior became erratic, non-continuous spatially [Fig. 7] nor temporally [Fig. 2]. The probability depth diagrams [Fig. 10.6] are no longer ordered by expectancy [Fig. 2.4] and are no longer concave [Fig. 2.2] nor continuous [Fig. 2.1]. These findings render the historical data and the stalwart design paradigm obsolete.

The physical database supporting the municipal drainage master plan [Fig. 12] was proven lacking, erroneous at part, and in general not representing the actual physical system [Fig. 17]. Further analysis attested to pathogens that were not treated, amounting to an avalanche and a loss of systemic teleonomic coherence [

Fig. 15]. The stalwart analytical tools used in the master plan were proven wrong, owing to morphology changes, interconnectivity with the sewerage and road systems, un-continuous flow in the drainage system (owing to phenomena such as bursts, air pockets, and of feeding to other systems), unaddressed complex modes of operation such as coupling and emergent traits such as pressure vessels.

In the case-study analyzed here, the municipal report center provided a window to the information system. It supplied a partial picture of the maintenance efforts captured by Date-time reports [*Fig. 8*]. The documented enormity of faults recurrence is by itself a testament to the vein efforts of maintenance efforts [Fig. 16.3].

Faults PDF was found to be lognormal. This finding is a manifestation of a general rule (Horvath, 1959) suggesting the machination of correlated faults. The Fast Fourier Transform of the Faults log [Fig. 3.2] shows erratic behavior with repetitive formations reminiscent of fractals.

The magnitude of faults was best fitted by a power function [Fig. 4] as provisioned by (Yonat & Shohet, 2022b). Power function is an indication of complexity. It implies a big quantity of small magnitude events and a small quantity of big magnitude events and a multitude of complex phenomena such as, the butterfly effect shown on Fig. 5 where at the end of the 2018 rain season, a rain of 2.5 mm thickness caused an avalanche. There were black swan phenomena such as the flooding portrayed on the ridge over the water divide line in the adjacent catchment basin [Fig. 19.3]. There were emergent traits such as conduits acting as pressure vessels thus flooding upper regions [Fig. 16.2], and the emergent of oscillators [Fig. 19.5]. The formation of loops creates higher topologies that are transient [Fig. 6.3], i.e.- different loops may be produced on different occasions. The free element of the power function equation represents constant "noise". It was shown that the noise is "white noise" [Fig. 14] as provisioned by the equation. The magnitude of the noise showed repetitive formations hinting to a recursive sub formations morphology. The origin of the noise was traced to a sagging of the sewage system that caused an unreversible damage to the drainage system [Fig. 15].

The power functions spatial manifestation was a recurring finding. It was presented on Fig. 16.4 for a spatial manifestation of a specific type of fault and by a Pareto diagram [Fig. 11.3] for an aggregated function of all faults. This shows that fractalized various responses are super positioned. The Pareto indicates that 90% of the faults recure in 20% of the locations. This attests to a phenomenon of attractors. An attractor was studied [Fig. 19], it was linked to upstream successive fluxes [Fig. 19.3] and a "black swan", of first time flooding a higher catchment. These effects were matched with an explanatory model [Fig. 19.4]. These effects are a product of design errors that might have been latent in the past, but now, having become active, "remedial" designs that offer to relieve the system by adding links to mains, must be rejected adamantly.

Spatio-temporal networks were produced from the municipal Fault log [such as Fig. 18]. The morphology shows repetitive structural formations and recursive sub formations. The morphology of the generated fault network is not similar to the physical morphology of the system [Fig. 12]. The noted physical morphology was proved lacking. Markedly, there are no notations of crossovers with the sewerage system, manhole heights, and inlets invert levels. The Virtual fault networks bypassed all systemic unknowns, changes, modifications and imported risk and related directly to the system's response. Fault networks suggested flows, directions, incorporated sewage, and roads, as well as flooding locations, identified attractors and highlighted hubs and emergent formations. This created spatio-temporal maps that needed to be evaluated against the physical maps to equate a meaning to the virtual findings. Pathogens, such as manholes' sagging, pressure vessels, air pockets, and many other products of maintenance deficiencies and design latent errors are hidden. In the case-study, descriptive statistics pinpointed a major event of sagging of the sewerage system, noted on Fig. 15, that changed the gradients, caused incessant clogging and a loss of operational and teleonomic coherence in the drainage system. The virtual networks were compared to the known physical data to derive an understanding and decipher the modus operandi of the actual system. It was found that the drainage system cannot drain the city within the timeline the city is drained, not even for the design rain thickness [Fig. 10]. It was found that an alternative drainage system is formed, using roads' gutters as conduits [Fig. 16.1].

DSP tools among many real time management tools are readily available. DSP tools were presented here for the management of the recesses and a for a suggested seasonal pond. It is paramount that the use of these tools is within a theoretical relevant model, in our case,- ToF. Whenever possible, simple low-tech solutions are advised. Simple mechanical low maintenance stand-alone contraptions are oftentimes better fitted to serve the systemic needs, such as a simple non-return mechanical valve to prevent the coupling effect of Fig. 19.5.

The deciphering of the rain characteristics and the system Modus Operandi were put to immediate use in the commissioning of a municipal meteorologic station, submission of a revised drainage master plan, the stoppage of a pending counter productive investment, and the suggested use of DSP and feedback controllers.

CONCLUSIONS

This paper introduces the application of the **T**heory **o**f **F**aults to analysis, design, management, and control of a CIS. It was suggested the physical CIS is a part and product of an information system. A fault log was analyzed to produce the trajectories of faults that propagate the systems and cause disruptions and morphological changes. These trajectories were tracked on the info-system spatio-temporal network. Local snapshots were presented. This spatio-temporal map is the system's response, it was generated without knowing the exact morphology, pathogens, and the rain spatio-temporal expression.

By comparing the virtual system to what is known of the physical one, design implication and real time management tools were employed.

It was shown that complex systems may be evaluated and managed as black boxes by analyzing system response. It was deduced that although the actual system morphology and pluvial flood risk are not known, system attractors and emergent behaviors may be discerned, and design corrections and real time management tool may be developed.

ACKNOWLEGMENTS

The authors express their indebtedness to BGU-NJIT joint research funding NJIT-BGU seed grants 2021- Civil and Environmental Engineering Grant No, 87894411.
The authors express their gratitude to SAGIE J.A.4 for its generous support.

APPENDIX

Rain

Spatial distribution

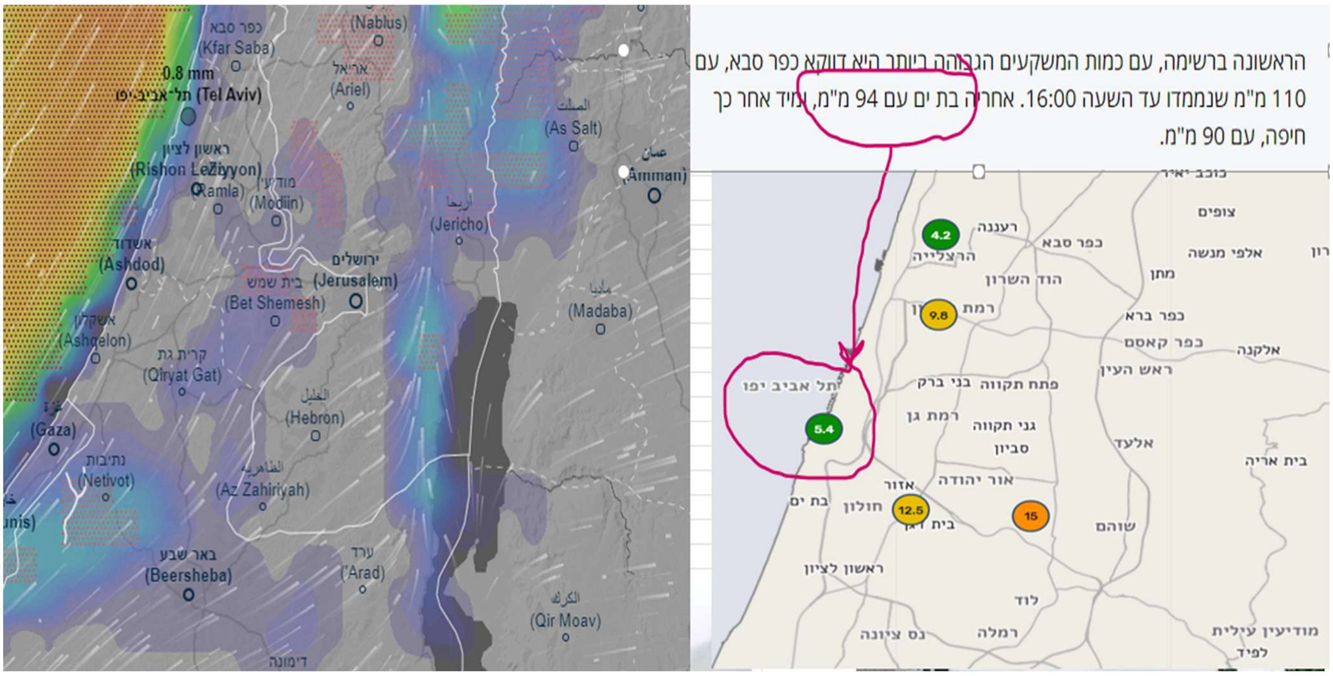

Fig. 7 Rain spatial distribution for the 19.11.2021 rainstorm. The upper red circle denotes the local rain thickness, the lower one in the thickness in the barometric station.

4 Sagie J.A. engineering and Construction LTD

Fault Log

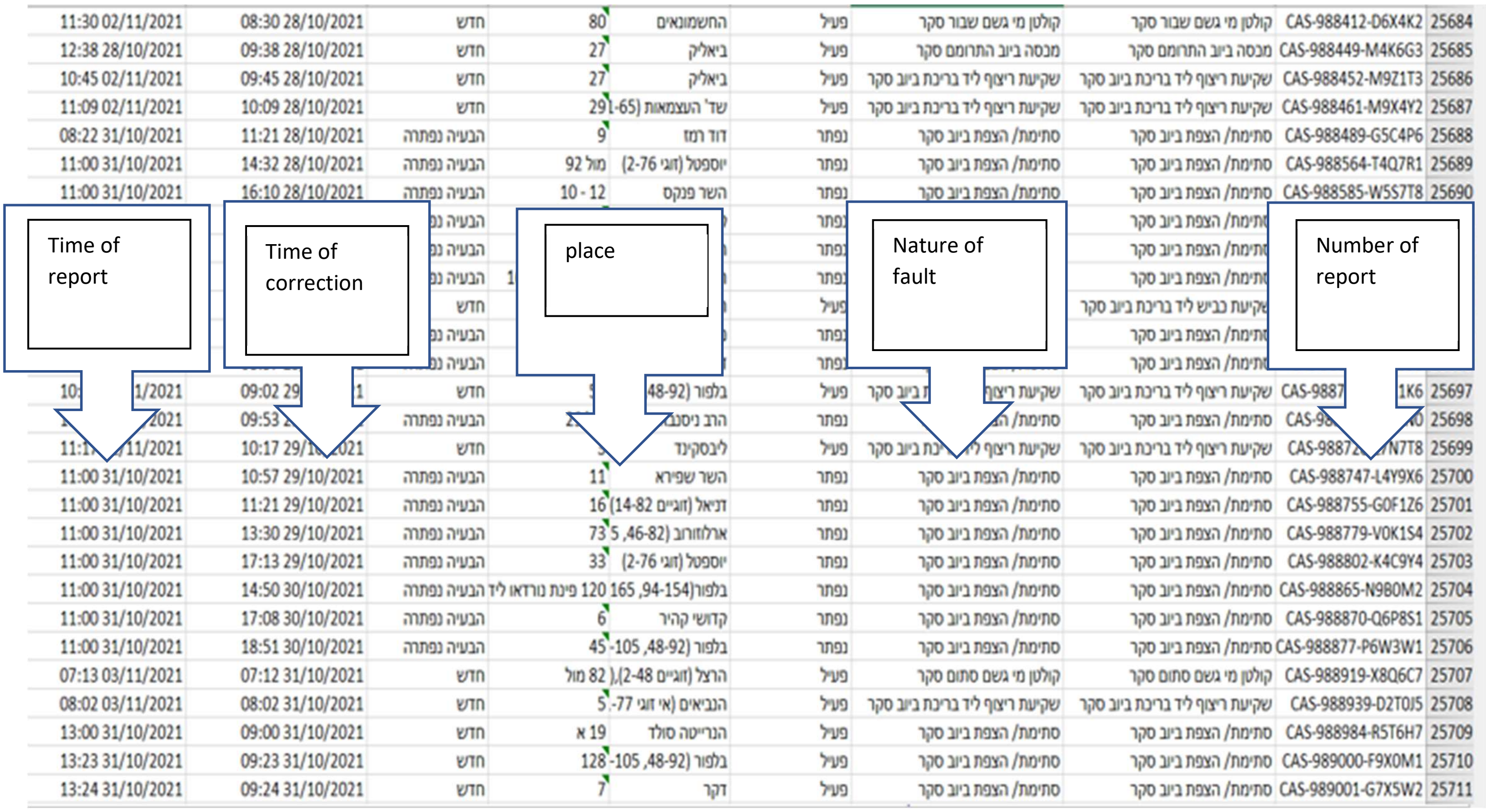

Fig. 8. Faults log-DateTime of opening of report, DateTime of closing, place,category

																							100	50	20	10	5										
						צינור קיים + נוסף		צנור נוסף		הפרש	צנור קיים		צנור מוצע			שיפוע	ספיקות בהסתברות שונה					עוצמות בהסתברות שונה					מקדם	זמן	שיפוע	T.L.2	T.L.1	אורך	שטח מצטבר	שטח	מס'	
						ספיקה	תוספת לנדרש	ספיקה	קוטר		ספיקה	קוטר	ספיקה	מהירות	קוטר	ממוצע	(1:5) 20%	(1:10) 10%	(1:20) 5%	(1:50) 2%	(1:100) 1%	(1:5) 20%	(1:10) 10%	(1:20) 5%	(1:50)2%	(1:100) 1%	נגר C	ריכוז				האפיק/קטע			נקודה	
עוצמה לפי זמן ריכוז עבור אזור 6						(מ"ק/שנ')	(ס"מ)	(מ"ק/שנ')	(ס"מ)		(מ"ק/שנ')	(ס"מ)	(מ"ק/שנ')	(מ/שנ')	(ס"מ)	(%)	(מ"ק/שניה)					(מ"מ/שעה)					(-)	(דק')	(%)	(מטר)	(מטר)	(מטר)	(דונם)	(דונם)		
I20%	I10%	I5%	I2%	I1%	זמן	1.49	-0.25	1.02	80	(0.11)	0.47	60	1.85	2.35	100	0.6	1.2	1.5	1.7	2.1	2.4	83	101	116	139	157	0.6	18	1.1%	20	25.75	512	90	90	A10.1-A10	
122	149	166	194	216	10	4.02	0.79	3.20	100	0.02	0.82	60	3.20	4.08	100	1.8	2.3	2.8	3.2	3.8	4.3	93	113	129	154	173	0.6	15	2.3%	20	33.5	588	150	150	A11-A10	1
93	113	129	154	173	15	5.05	-1.27	3.87	125	0.02	1.18	80	6.30	3.57	150	0.8	4.5	5.5	6.3	7.6	8.6	79	97	112	134	152	0.6	19	1.4%	14.8	20	380	340	100	A10-A8	1
76	93	107	130	147	20	6.00	-0.34	3.87	125	0.04	2.13	100	6.30	3.57	150	0.8	4.5	5.5	6.3	7.7	8.7	76	93	107	130	147	0.6	20	0.1%	14.65	14.8	165	355	15	A8-A7	1
58	71	83	103	118	30	7.04	0.34		-	(0.34)	7.04	150	7.04	3.99	150	1.0	4.7	5.8	6.7	8.1	9.2	76	93	107	130	147	0.6	20	2.8%	12.15	14.65	90	375	20	A7-A6	1
44	53	64	81	94	45	5.91	-1.77	0.93	80	(0.42)	4.98	150	8.10	3.19	180	0.5	5.4	6.6	7.7	9.3	10.6	72	88	102	124	141	0.6	22	0.0%	12	12.15	320	450	75	A6-A5	1
						0.00	0.00			-																										1
עוצמה לפי זמן ריכוז עבור אזור 6						2.02	-0.36	1.38	80	(0.12)	0.64	60	2.50	3.19	100	1.1	1.7	2.0	2.4	2.9	3.3	67	82	95	116	133	0.6	25	1.6%	25.3	41.51	1000	150	150	A5.8-A5.7	1
I20%	I10%	I5%	I2%	I1%	זמן	4.05	-0.59	2.61	100	(0.10)	1.44	80	4.74	3.87	125	1.2	3.3	4.0	4.6	5.7	6.5	65	79	93	113	130	0.6	26	3.1%	14.55	25.3	345	300	150	A5.7-A5.2	1
122	149	166	194	216	10	4.37	-0.76	3.35	125	(0.33)	1.02	80	5.45	3.09	150	0.6	3.6	4.4	5.1	6.3	7.2	63	77	91	111	127	0.6	27	1.1%	12	14.55	235	340	40	A5.2-A5	1
116	142	159	186	207	11	16.63	4.08			(0.01)	16.63	200	12.55	4.94	180	1.2	8.8	10.7	12.5	15.3	17.4	67	82	95	116	133	0.6	25	2.2%	1	12	500	790	0	A5-A0	1
110	134	151	178	199	12					-																										1
104	127	144	170	190	13	4.24	0.95	3.37	100	(0.08)	0.86	60	3.37	4.30	100	2.0	2.3	2.9	3.3	4.0	4.5	79	97	112	134	152	0.6	19	2.3%	28.47	47.15	805	177	177	B10-4.4-B10-4	1
99	120	136	162	182	14	6.68	-1.49	5.12	125	(0.17)	1.56	80	8.33	4.72	150	1.4	5.8	7.1	8.2	9.9	11.2	76	93	107	130	147	0.6	20	2.7%	13.8	28.47	540	457	280	B10-4 - B10-1	1
93	113	129	154	173	15	7.89	-1.28	5.89	150	(0.42)	2.00	100	9.59	3.77	180	0.7	6.5	7.9	9.2	11.1	12.6	74	90	105	127	144	0.6	21	1.2%	11.6	13.8	180	525	68	B10-1 - B10	1
89	109	125	149	168	16	18.17	3.49	11.25	180	(0.23)	6.92	150	14.91	4.75	200	1.0	10.4	12.6	14.7	17.8	20.2	72	88	102	124	141	0.6	22	1.0%	10.25	11.6	140	860	335	B10-B9	1
86	105	120	144	163	17	15.48	-2.20	9.59	180	(1.02)	5.89	150	18.70	4.99	250/150	0.7	12.5	15.2	17.7	21.4	24.4	72	88	102	124	141	0.6	22	0.5%	8.81	10.25	265	1036	176	B9-B8	1
83	101	116	139	157	18	17.33	-2.81	8.10	180	(2.70)	9.23	170/150	22.84	4.95	250/200	0.5	14.2	17.3	20.1	24.5	27.8	70	86	100	121	138	0.6	23	0.6%	8.26	8.81	100	1208	172	B8-B7	1
79	97	112	134	152	19	19.96	-1.34	10.73	200	(1.53)	9.23	170/150	22.84	4.95	250/200	0.5	15.0	18.3	21.3	25.9	29.5	70	86	100	121	138	0.6	23	1.0%	8.35	8.26	120	1278	70	B7-B6	1
76	93	107	130	147	20	21.87	-1.36	11.76	200	(1.85)	10.11	170/150	25.08	4.95	250/200	0.6	16.3	19.9	23.2	28.3	32.3	67	82	95	116	133	0.6	25	0.2%	7.55	8.35	420	1463	185	B6-B4	1
74	90	105	127	144	21	21.87	-2.95	11.76	200	(0.26)	10.11	170/150	25.08	5.01	250/200	0.6	17.4	21.2	24.8	30.2	34.5	67	82	95	116	133	0.6	25	0.6%	6.9	7.55	100	1563	100	B4-B3	1
72	88	102	124	141	22	38.51	9.95	26.13	250	(2.07)	12.38	170/150	30.64	6.12	250/200	0.9	20.0	24.4	28.6	34.9	39.9	65	79	93	113	130	0.6	26	2.0%	1	6.9	300	1845	282	B3-B0	1
70	86	100	121	138	23					-																										1
69	84	98	119	135	24	3.00	-0.21	2.39	100	(1.12)	0.61	60	4.33	3.53	125	1.0	2.3	2.8	3.2	3.8	4.3	86	105	120	144	163	0.6	17	1.8%	29.26	40.44	614	160	160	2.1	1
67	82	95	116	133	25	3.00	-0.66	2.39	100	(0.67)	0.61	60	4.33	3.53	125	1.0	2.7	3.3	3.7	4.3	4.8	110	134	151	178	199	0.6	12	2.5%	35.2	47.2	476	145	145	2.2	
65	79	93	113	130	26	7.65	-0.21	4.93	125	(0.17)	2.72	100	8.03	4.55	150	1.3	5.5	6.7	7.9	9.6	10.9	67	82	95	116	133	0.6	25	2.2%	23.85	47.63	1100	495	495	2.3	2
63	77	91	111	127	27	3.88	-0.62	2.50	100	(0.04)	1.38	80	4.54	3.70	125	1.1	3.1	3.8	4.5	5.5	6.3	60	73	86	105	121	0.6	29	1.6%	19.8	39.9	1220	315	315	2.4	2
61	75	88	108	124	28	6.58	0.70	3.29	100	(0.09)	3.29	100	5.97	4.86	125	1.9	4.1	5.0	5.9	7.2	8.2	67	82	95	116	133	0.6	25	2.2%	18.28	40.42	986	370	370	2.5	2
60	73	86	105	121	29	5.32	0.27	1.24	80	(1.59)	4.08	125	6.64	3.76	150	0.9	3.5	4.3	5.1	6.2	7.2	55	67	80	98	113	0.6	33	0.9%	19.5	28.8	1045	381	381	2.6	2
58	71	83	103	118	30					-																										2
57	69	82	101	116	31	3.41	-1.42	2.72	100	(0.10)	0.70	60	4.93	4.02	125	1.3	3.4	4.2	4.8	5.8	6.6	79	97	112	134	152	0.6	19	4.8%	21.86	30	170	260	260	C10-C9	2
56	68	81	100	115	32	6.99	1.19	5.89	150	(0.09)	1.10	80	5.89	3.34	150	0.7	4.1	5.0	5.8	7.0	8.0	76	93	107	130	147	0.6	20	0.9%	21	21.86	92	325	65	C9-C8	
55	67	80	98	113	33	6.00	-0.27	3.87	125	(0.03)	2.13	100	6.30	3.57	150	0.8	4.4	5.4	6.3	7.6	8.7	67	82	95	116	133	0.6	25	1.2%	18	21	250	395	70	C8-C7	3
54	66	78	97	112	34	7.89	-1.19	5.89	150	(0.51)	2.00	100	9.59	3.77	180	0.7	6.4	7.8	9.1	11.0	12.5	72	88	102	124	141	0.6	22	1.0%	17	18	100	532	137	C7-C6	3
53	65	77	95	110	35	8.94	-1.76	6.68	150	(0.17)	2.26	100	10.87	4.27	180	0.9	7.6	9.2	10.7	13.0	14.8	72	88	102	124	141	0.6	22	0.3%	16	17	387	627	95	C6-C5	3
52	64	76	94	108	36	8.14	-5.24	3.87	125	(0.20)	4.27	2x100	13.58	4.32	200	0.8	9.5	11.6	13.4	16.2	18.4	76	93	107	130	147	0.6	20	0.4%	15	16	250	749	122	C5-C4	3
51	62	75	92	107	37	14.04	-3.86	6.30	150	(1.39)	7.74	2x125	19.30	5.29	250/150	0.8	12.6	15.4	17.9	21.7	24.7	72	88	102	124	141	0.6	22	1.3%	13	15	155	1049	300	C4-C3	3
50	61	73	91	105	38	20.38	-1.66	10.87	180	0.83	9.51	150/140	21.21	5.65	250/150	0.9	15.6	19.0	22.0	26.7	30.4	72	88	102	124	141	0.6	22	1.0%	7	13	589	1291	242	C3-C1	3
49	60	72	90	104	39	21.92	-4.18	10.25	180	(2.79)	11.67	170/150	28.89	5.78	250/200	0.8	18.5	22.5	26.1	31.5	35.8	76	93	107	130	147	0.6	20	3.3%	1	7	180	1461	170	C1-C0	3
48	59	71	88	102	40																			3,624									22307			3
47	58	69	87	100	41																															3
47	57	68	85	99	42																															
46	56	67	84	97	43																															
45	54	66	82	96	44																															
44	53	64	81	94	45																															

15.48	3.44	250/200	0.3	0.3
8.61	2.97	200/160	0.3	0.3
2.47	1.96	140/100	0.3	0.3
2.85	2.27	140/100	0.4	0.4
5.73	2.25	180	0.25	0.25
3.52	1.99	150	0.25	0.25
3.86	2.18	150	0.3	0.3
4.45	2.52	150	0.4	0.4

ספיקה	מהירות זרימה	שיפוע אורכי	רדיוס מורטב	היקף מורטב	שטח מורטב	גובה	רוחב
			[m]	P [m]	[m]	[cm]	[cm]
23.45	5.21	1	0.69	6.5	4.5	200	250
9.66	4.21	1	0.50	4.56	2.295	150	170
7.50	3.97	1	0.46	4.1	1.89	140	150
13.47	4.62	1	0.58	5.04	2.916	180	180
15.30	4.53	1	0.56	6	3.375	150	250

קוטר איקוויוולנטי	שני צנורות	שטח חתך	קוטר צינור
85	0.57	0.28	60
113	1.00	0.50	80
141	1.57	0.79	100
177	2.45	1.23	125
212	3.53	1.77	150

Fig. 9. Hydrological data supplied in the general municipal drainage plan.

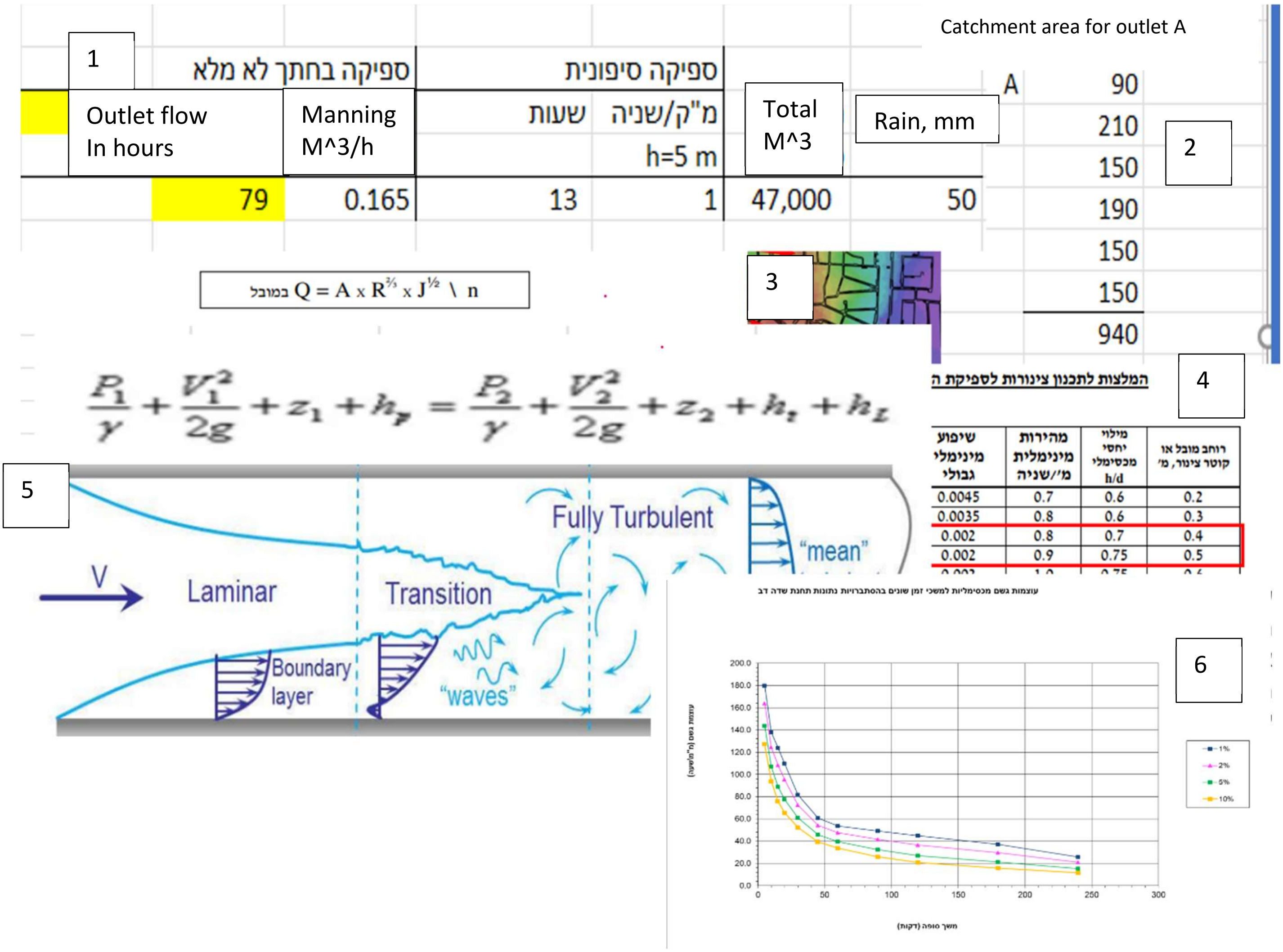

Fig. 10. Hydrological considerations based on Manning and Bernoulli and Kirpich equations enables a gross estimate of the total capacity of the stormwater system capitalizing on the fact that there is only one outlet for the western sub-systems.

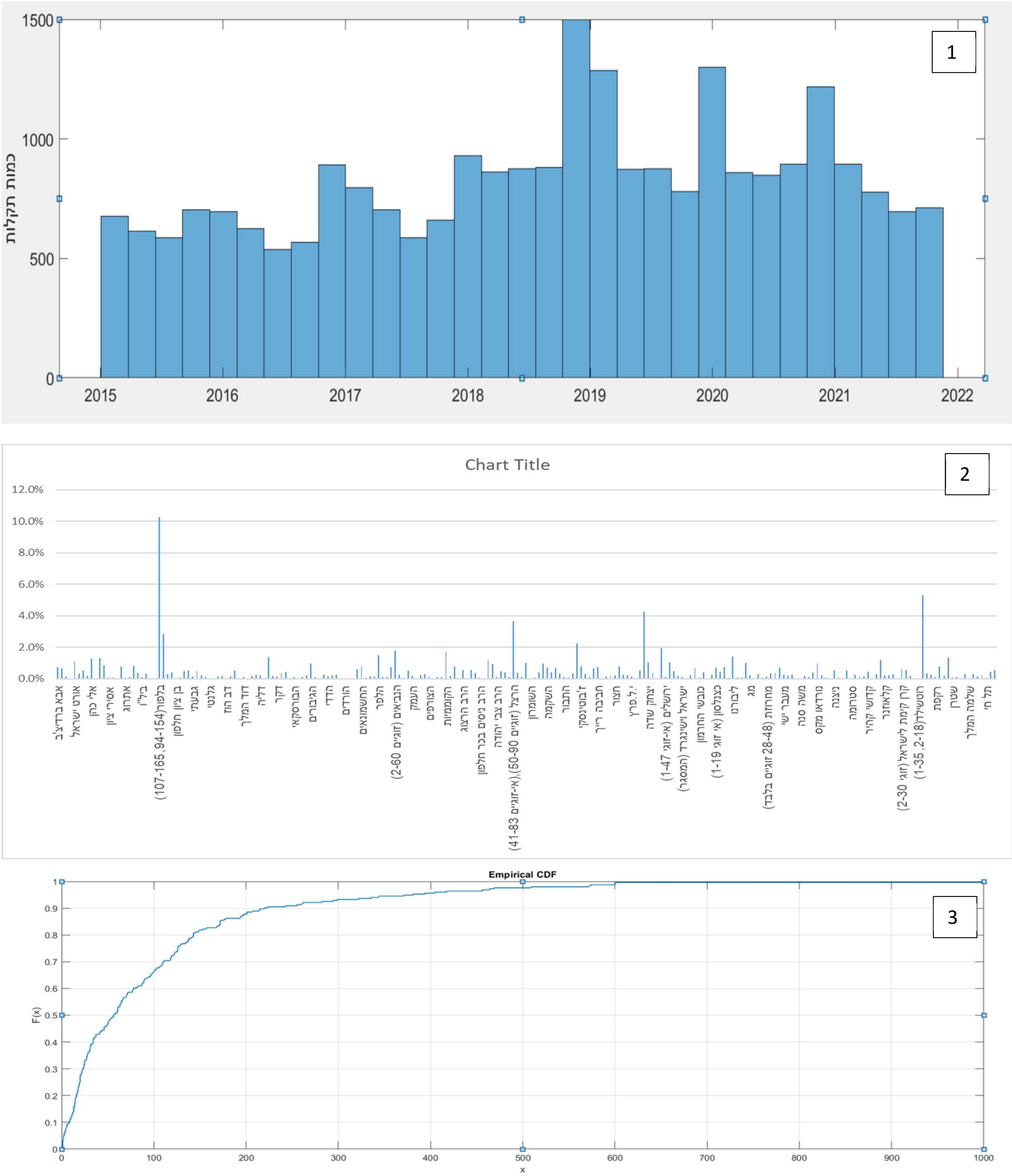

*Fig. 11. (*1)Timeline of quantity of faults, (2)percentage and (3)Pareto of faults per location

Physical data

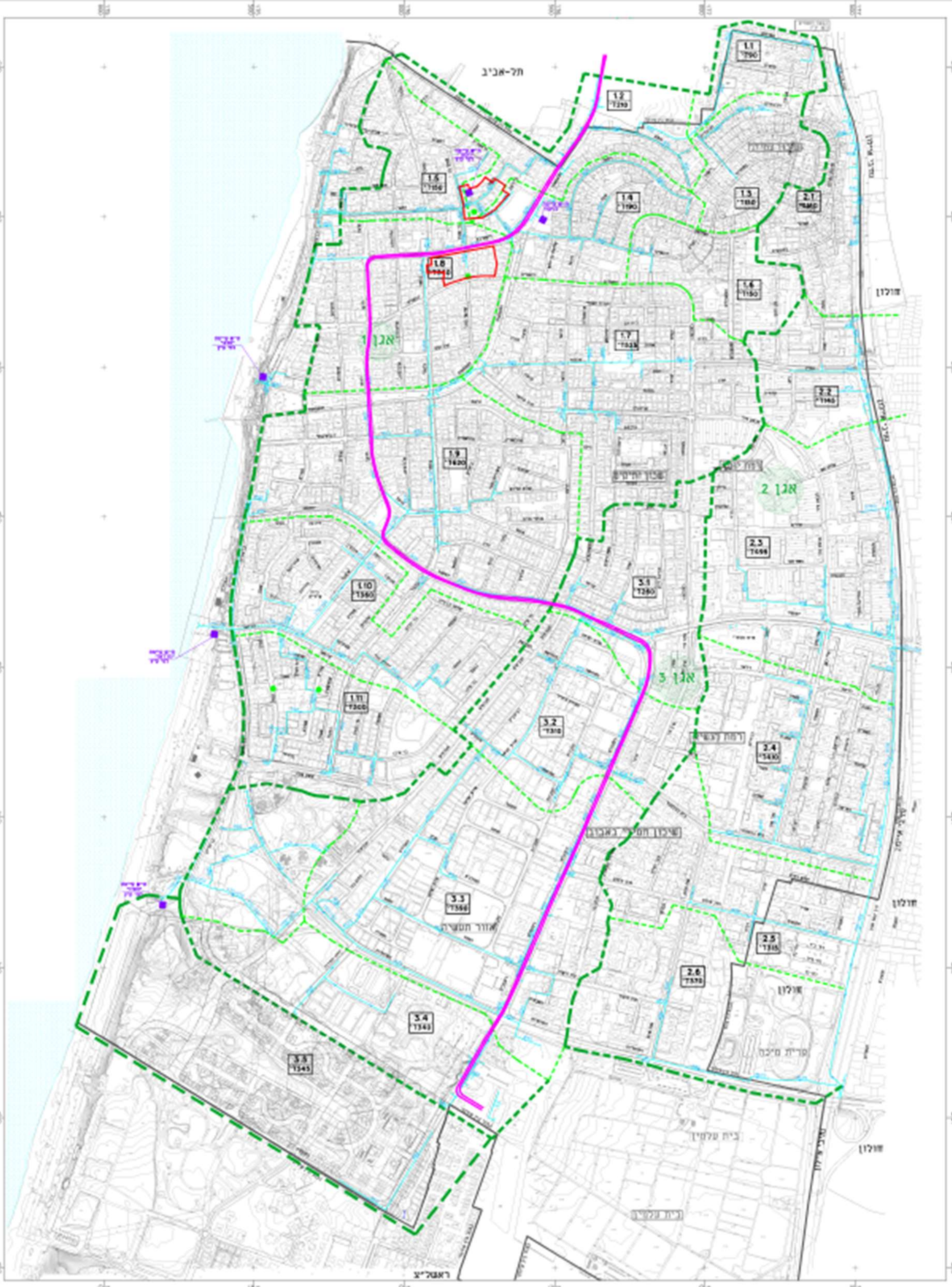

Fig. 12 "As is" physical system

Topography

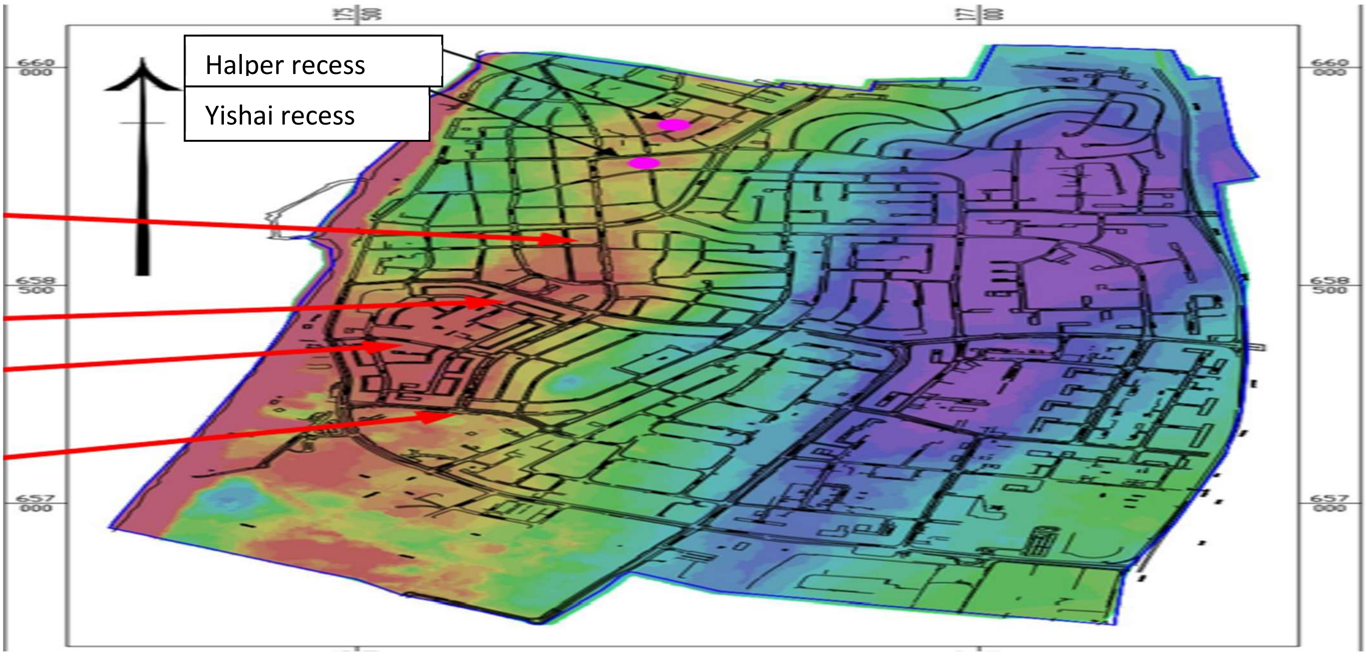

Fig. 13. Topography

White noise

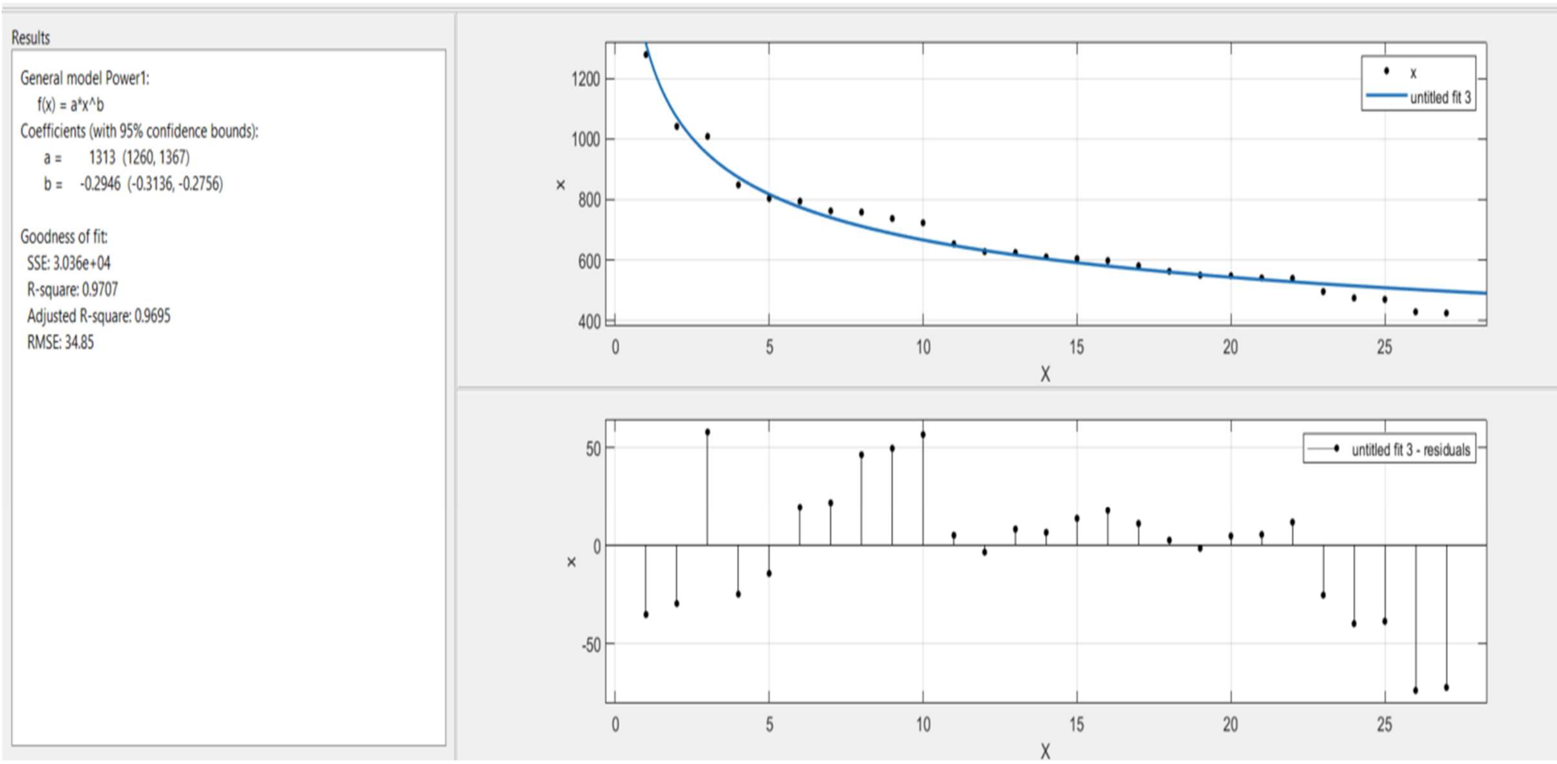

Fig. 14. White noise power function and White noise formation, showing repetitive formations that are not related to the magnitude

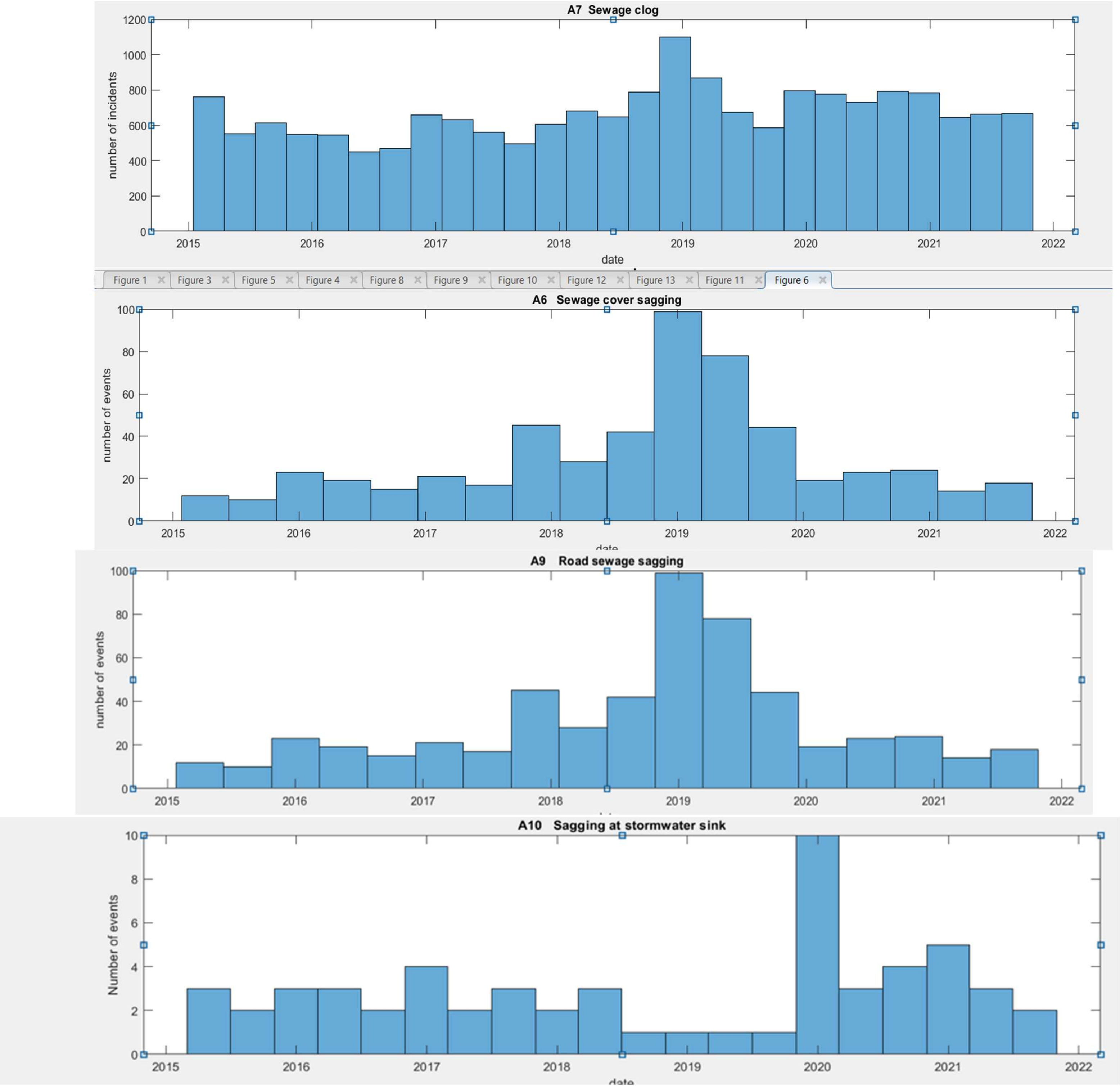

Fig. 15. The cause of the White noise

Physical forensics

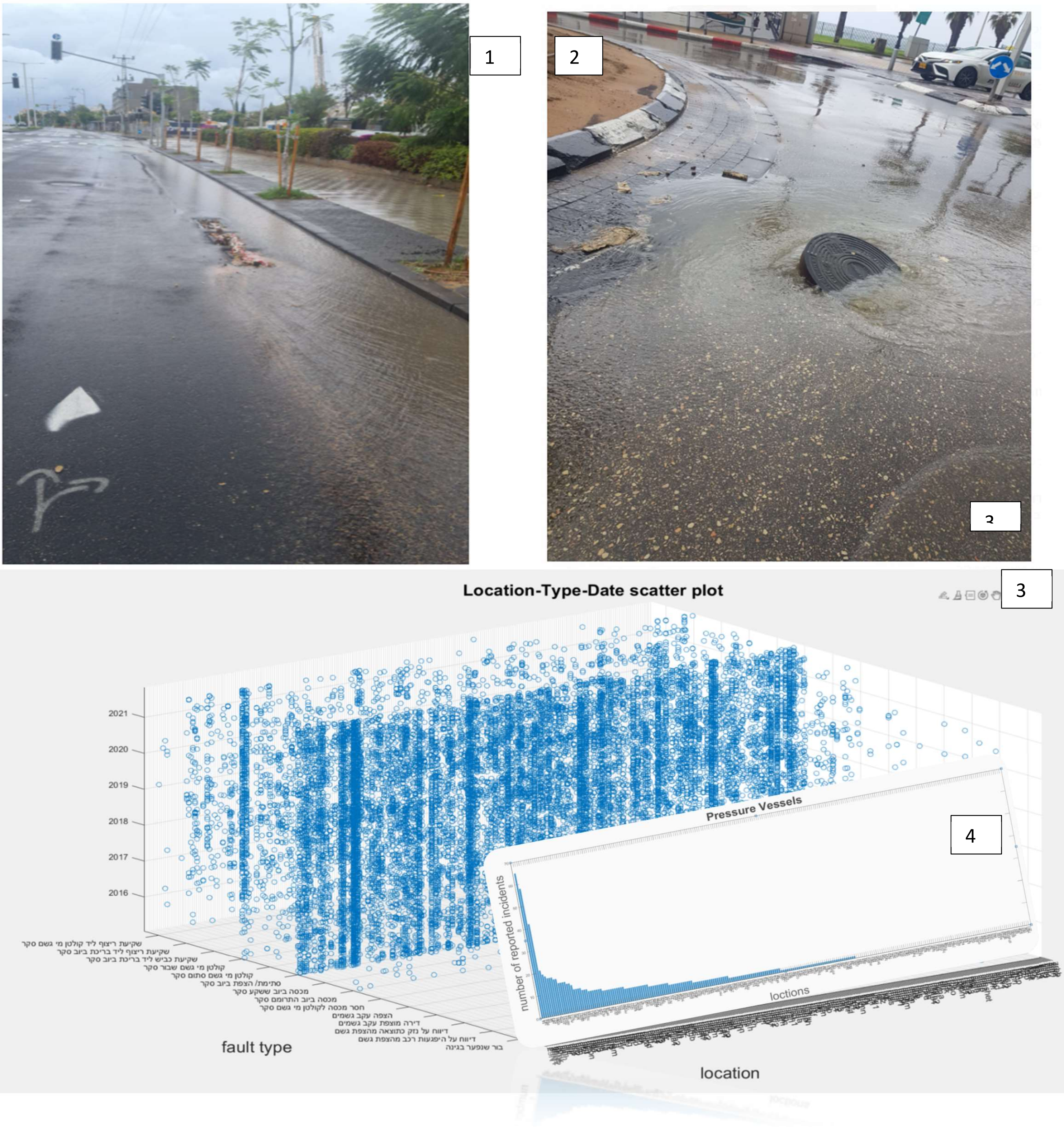

Fig. 16. Physical findings. (1) the actual drainage transfer system, (2) a pressure conduit burst a few km uphill (3)3D scatter plot of faults (4)number of reported incidents of top burst per location.

Sewage discharge, water contamination, impairment to sewage systems.
Trapped air effect (Zhou et al., 2004).

Fig. 17. Physical findings

Morphology

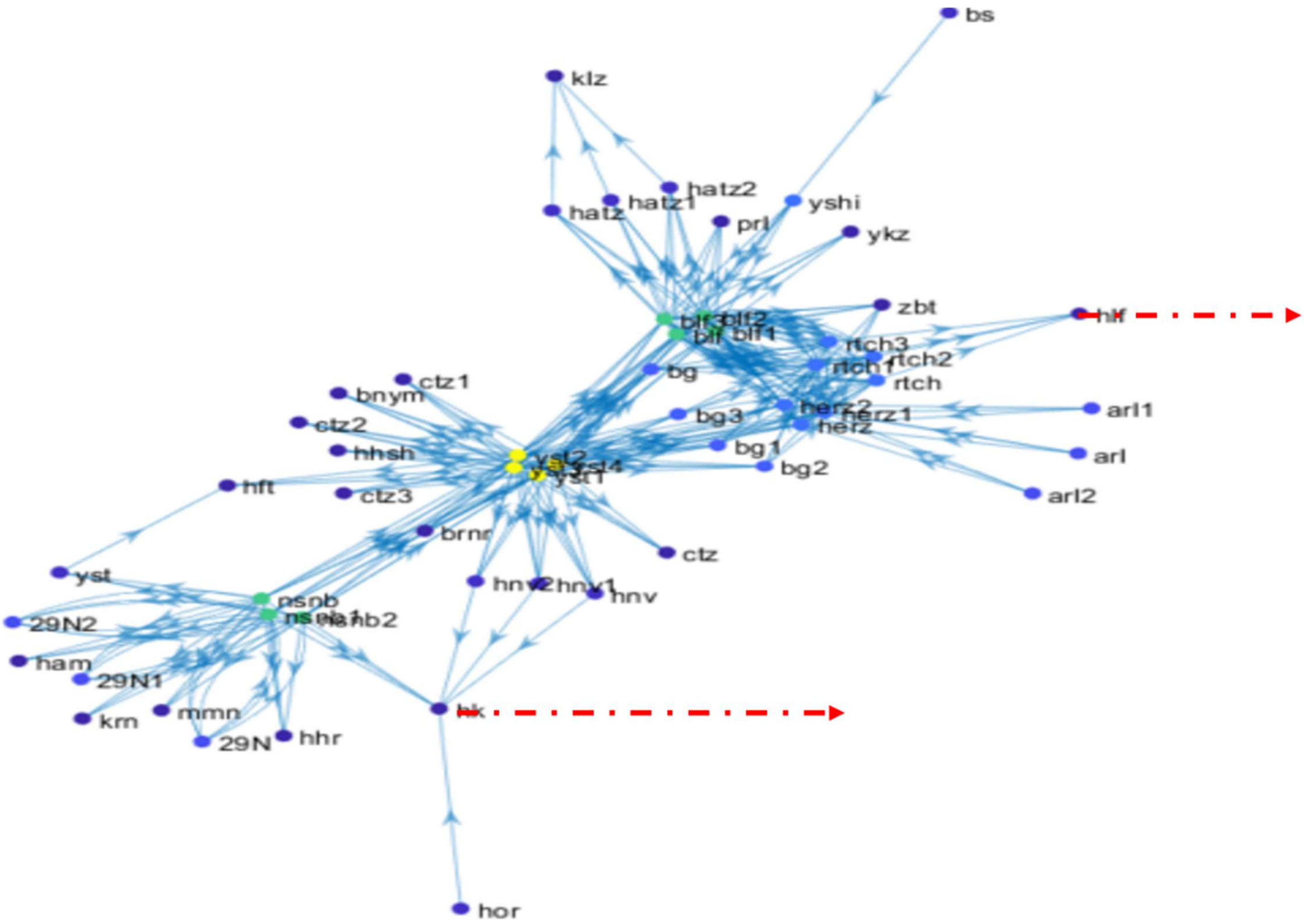

Fig. 18 Fault network general morphology of the western basin. The hydrological characteristics of the red outlets are given on Fig. 9

Betweenness centrality may be an indicator for Criticality Index.

attractors

Red arrows point to points of an attractors

Attractors are nodes of the network.

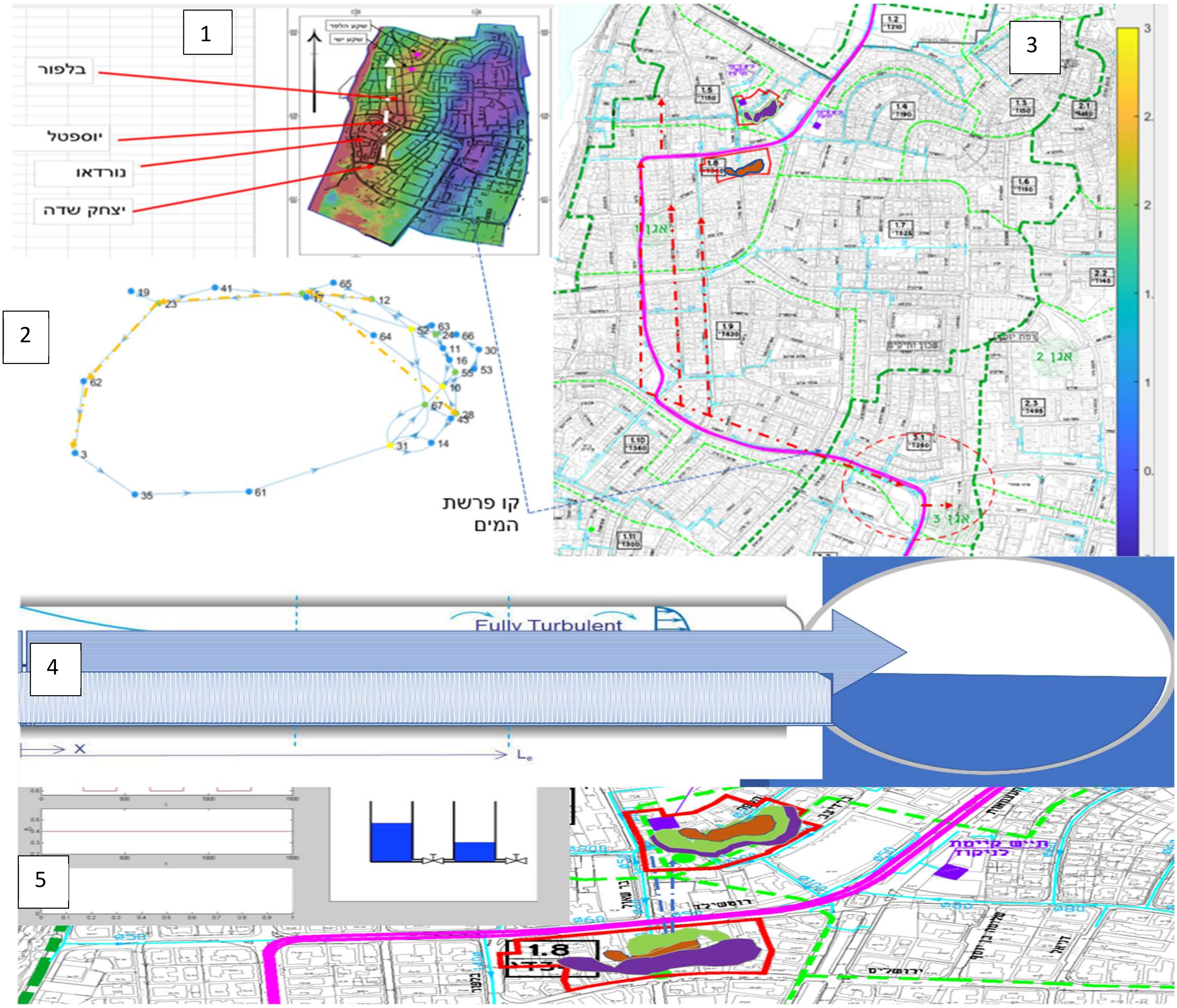

Fig. 19. (1) topographical overview (2) a spatio-temporal fault map that is a Zoom-in into (3) a portion of the physical net showing against gradient flows. (4) a suggested explicatory model, and (5) a possible oscillator.

PID Controller

Aseasonal pond is suggested.

Fig. 20. Suggested seasonal pond, ingress and overflow

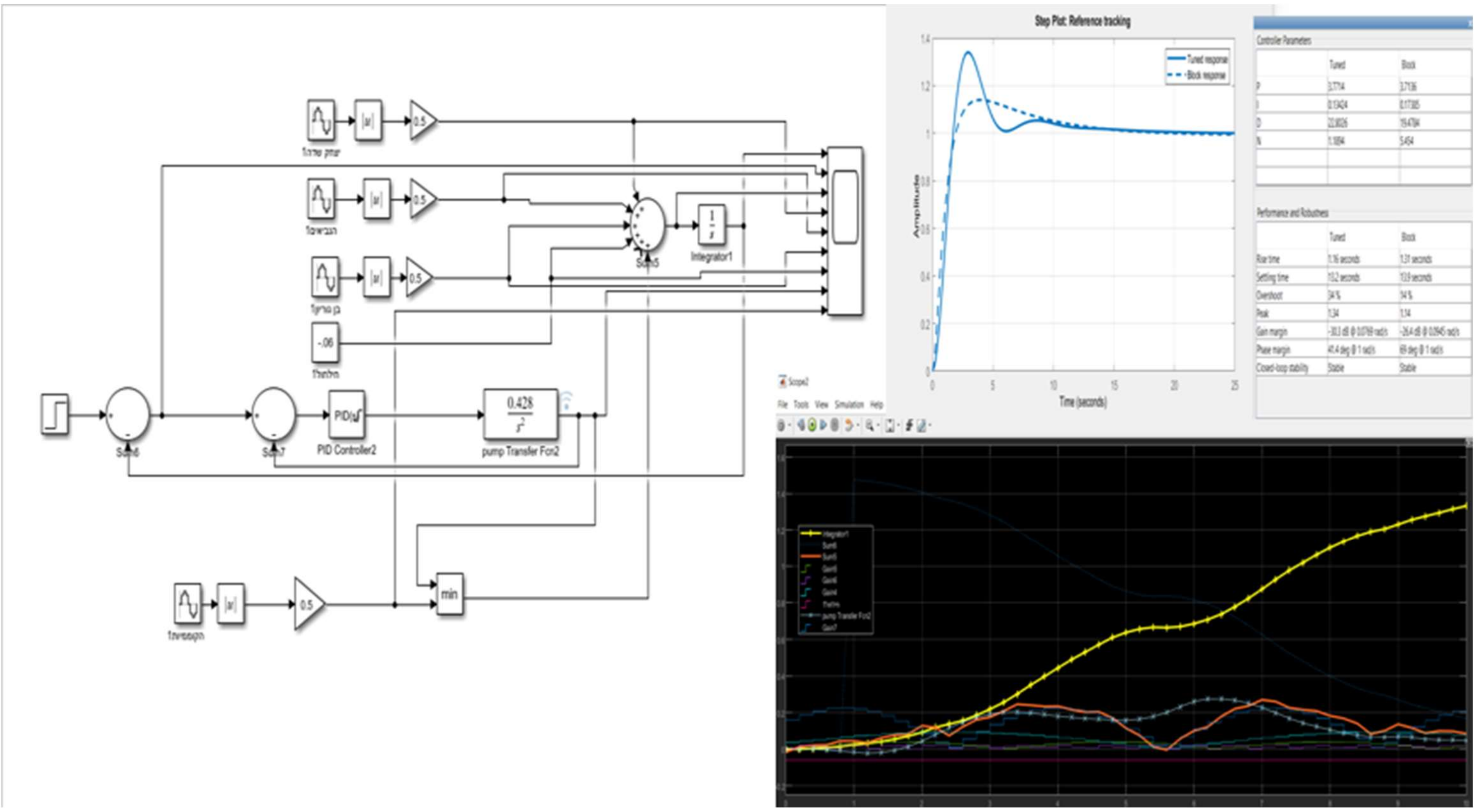

Fig. 21. PID system, parameters and controlled output

REFERENCES

References

Apan, A., & McDougall, K. (2015). Vulnerability assessment and interdependency analysis of critical infrastructures for climate adaptation and flood mitigation. *International Journal of Disaster Resilience in the Built Environment,*

Araya, F., & Vasquez, S. (2022). Challenges, drivers, and benefits to integrated infrastructure management of water, wastewater, stormwater and transportation systems. *Sustainable Cities and Society, 82*, 103913.

Arfa, S., Nasseri, M., & Tavakol-Davani, H. (2021). Comparing the effects of different daily and sub-daily downscaling approaches on the response of urban Stormwater collection systems. *Water Resources Management, 35*(2), 505-533.

Aronica, G. T., & Lanza, L. G. (2005). Drainage efficiency in urban areas: a case study. *Hydrological Processes: An International Journal, 19*(5), 1105-1119.

Duan, Z., Tuo, Y., Liu, J., Gao, H., Song, X., Zhang, Z., Yang, L., & Mekonnen, D. F. (2019). Hydrological evaluation of open-access precipitation and air temperature datasets using SWAT in a poorly gauged basin in Ethiopia. *Journal of Hydrology, 569*, 612-626.

Fitobór, K., Ulańczyk, R., Kołecka, K., Ramm, K., Włodarek, I., Zima, P., Kalinowska, D., Wielgat, P., Mikulska, M., & Antończyk, D. (2022). Extreme weather layer method for implementation of nature-based solutions for climate adaptation: Case study Słupsk. *Science of the Total Environment, 842*, 156751.

The European Parliament and the Council of European Union, Official Journal of the European Communities, 2000, 01–73. 60, Council of 23 October 2000Cong. (2000). https://eur-lex.europa.eu/legal-content/EN/TXT/?uri=celex%3A32000L0060

Gironás, J., Roesner, L. A., Rossman, L. A., & Davis, J. (2010). A new applications manual for the Storm Water Management Model(SWMM). *Environmental Modelling & Software, 25*(6), 813-814.

Horvath, W. J. (1959). Applicability of the lognormal distribution to servicing times in congestion problems. *Operations Research, 7*(1), 126-128.

Johansson, J., & Hassel, H. (2010). An approach for modelling interdependent infrastructures in the context of vulnerability analysis. *Reliability Engineering & System Safety, 95*(12), 1335-1344. rg/10.1016/j.ress.2010.06.010

Jung, M., Kim, H., Mallari, K., Pak, G., & Yoon, J. (2015). Analysis of effects of climate change on runoff in an urban drainage system: a case study from Seoul, Korea. *Water Science and Technology, 71*(5), 653-660.

Kabir, G., Balek, N. B. C., & Tesfamariam, S. (2018). Consequence-based framework for buried infrastructure systems: A Bayesian belief network model. *Reliability Engineering & System Safety, 180*, 290-301.

Kändler, N., Annus, I., & Vassiljev, A. (2022). Controlling peak runoff from plots by coupling street storage with distributed real time control. *Urban Water Journal, 19*(1), 97-108.

Livius, T. (AD17). *Livy's History of Rome: Book 1*

Mourad, M., Bertrand-Krajewski, J., & Chebbo, G. (2006). *Design of a retention tank: comparison of stormwater quality models with various levels of complexity*. IWA Publishing. 10.2166/wst.2006.582

Mugume, S. N., Gomez, D. E., Fu, G., Farmani, R., & Butler, D. (2015). A global analysis approach for investigating structural resilience in urban drainage systems. *Water Research, 81*, 15-26.

Mullapudi, A., Wong, B. P., & Kerkez, B. (2017). Emerging investigators series: building a theory for smart stormwater systems. *Environmental Science: Water Research & Technology, 3*(1), 66-77.

Reason, J. (1995). Understanding adverse events: human factors. *BMJ Quality & Safety, 4*(2), 80-89.

Reason, J. (2000). Human error: models and management. *Bmj, 320*(7237), 768-770. https://www.bmj.com/content/320/7237/768.full

Salman, B. (2010). *Infrastructure management and deterioration risk assessment of wastewater collection systems*. University of Cincinnati.

Valizadeh, N., Shamseldin, A. Y., & Wotherspoon, L. (2019). Quantification of the hydraulic dimension of stormwater management system resilience to flooding. *Water Resources Management, 33*(13), 4417-4429.

Yonat, N., & Shohet, I. M. (2022a). *CPM Stability in Complex Projects and Systems*. Open Engineering Inc. 10.31224/2562

Yonat, N., & Shohet, Y. (2022b). Theory of Faults (ToF): Digital Statistic Quality Control in Complex Systems.https://doi.org/10.31224/2389

Yu, J., Qin, X., Chiew, Y. M., Min, R., & Shen, X. (2017). A stochastic optimization model for supporting urban drainage design under complexity. *Journal of Water Resources Planning and Management, 143*(9)

Zhou, F., Hicks, F., & Steffler, P. (2004). Analysis of effects of air pocket on hydraulic failure of urban drainage infrastructure. *Canadian Journal of Civil Engineering, 31*(1), 86-94.